


Enhancing soil conservation, water balance, and sediment yield in northern Morocco: A soil and water assessment tool model approach

Soufiane Aafir^{1*}, Abdessalam Ouallali², Mohamed Moukhchane³, Younes Laabdi⁴, Zineb Aafir⁵, Hamza Briak⁶, Lahsen Boudlal⁷, Habiba Aassoumi¹, Mohamed Beroho⁸

¹ Faculty of Sciences, Abdelmalek Es-saâdi University, Tetouan, Morocco

² Faculty of Sciences and Techniques of Mohammedia, Hassan II University of Casablanca, Mohammedia, Morocco

³ Higher Normal School of Tetouan, Abdelmalek Essaadi University, Tetouan, Morocco

⁴ Faculty of Sciences, Ibn Tofail University, Kenitra, Morocco

⁵ Faculty of Sciences of Rabat, Mohammed V University, Rabat, Morocco

⁶ College of Agriculture and Environmental Sciences, Mohammed VI Polytechnic University (UM6P), Bengueurir, Morocco

⁷ Maroc Ingenov, 83, Avenue Houmane Al Fatouaki, Aviation, Rabat 10000, Morocco

⁸ Faculty of Sciences and Techniques of Tangier, Abdelmalek Essaadi University, Tangier, Morocco

* Corresponding author's e-mail: soufianeaafir@gmail.com

ABSTRACT

Morocco is facing an alarming decline in surface water supplies, which is severely impacting dam reserves due to climate change and a scarcity of rainfall. The El Makhazine dam, located in the north, is crucial in supplying 800 Mm³ annually of water, and the irrigation of 34,000 ha in the Loukkos perimeter. The study and monitoring of water and sediment discharge are urgently needed to plan anti-erosion interventions, thus ensuring the sustainability of regional water resources. This study has achieved innovation by applying the soil and water assessment tool (SWAT) model to the basin using high-resolution data. These data include climate, flow, and sediment concentration from 1979 to 2019, topographic data, land use data from a high-resolution Sentinel image, and soil data from laboratory analyses. The SUFI2 algorithm was used to simulate the hydrological process in the basin. In contrast, the SWAT-CUP program calibrated and validated the model over two distinct intervals (1979–2002 and 2003–2019). The model utilized 23 sensitivity parameters to control flows and sediments, assessing reliability through statistical indices such as NSE, PBIAS, and R². The results were used to analyze the basin's water yield and calculate the water balance, revealing a predominance of evapotranspiration and surface runoff. Erosion rates and sediment load ranged from 5.36 to 99.86 t/ha/yr, with an average of 29.33 t/ha/yr. The sub-watersheds were prioritized and ranked based on their erosion rates, with a focus on implementing erosion control interventions. The results of the Best Management Practices simulation indicated that terracing was the most effective practice for the region, resulting in a 64.8% reduction in erosion. The model has demonstrated effectiveness in simulating watershed development and simulating practices to reduce dam siltation. This document is a valuable guide for planners in hydrological management in northern Morocco.

Keywords: sediment load, water balance, BMPs, soil conservation, SWAT model, north Morocco.

INTRODUCTION

Over time, the world has undergone significant demographic and economic evolution, resulting in increased pressure on the environment and a growing demand for natural resources, food, energy, and other essentials (O'Sullivan,

2020). The hydrological cycle, a fundamental component for sustaining life on Earth, is also influenced by economic development (Rast et al., 2014). Even a minor disruption of this cycle has detrimental effects on water and soil resources, thereby impacting food security (Ravi et al., 2010; Patra et al., 2023; Ologunde et al., 2024).

Understanding the hydrological cycle at a watershed scale provides better guidance for sustainable interventions and preservation efforts related to soils and water (Pande et al., 2020; Yang et al., 2021). Consequently, watershed-level interventions are now part of current strategies to combat soil degradation, water quality deterioration, and the reduction of water storage capacity in rivers and reservoirs.

Scientists consistently employ cutting-edge technologies when assessing hydrological cycles in watersheds. These technologies enable the rapid mapping of sediment-contributing areas, the estimation of water balance components within a watershed, and the quantification of the volume of water and sediment reaching the outlet (Li et al., 2021; Goharrokhi et al., 2022). Over time, all models developed have undergone improvements or have been used as a reference for creating new models. There is no perfect model for precisely simulating hydrological systems in watersheds. The choice of which model to apply primarily depends on local basin conditions, climatic and environmental parameters, and, most importantly, the availability of essential data for model implementation. In addition, some limitations and advantages vary from one model to another (Parra et al., 2018; Al-hasn et al., 2024). Review articles demonstrate that empirical models, such as USLE and its revised versions, RUSLE and modified MUSLE, are valid for estimating sheet erosion rates (Sadeghi et al., 2014; Djoukbala et al., 2019; Ketema and Dwarakish, 2021). None of these models considers parameters related to sediment load transported in gullies and streams. In contrast, the Potential Erosion Method (EPM) employs nearly the same parameters as the empirical USLE models, except that it considers erosion forms such as gullies, rills, bank cutting, and others (Ahmadi et al., 2020; Eltaif et al., 2022).

Sampling-based techniques have also been developed for soil assessment. These techniques typically rely on measuring radionuclides such as Cs-137, Pb-210, B-7, or magnetic susceptibility (Matisoff, 2014; Walling and Foster, 2016; Banerji et al., 2022). They enable the evaluation of soil degradation status and erosion degree with precision surpassing empirical models. However, they need to offer the capability to model the hydrological system within a watershed or quantify sediment load transport to the outlet (Ouallali et al., 2020).

The behavior of hydrological systems, including the water cycle, precipitation, river flow, and

sediment input, can be simulated using hydrological models (Santos et al., 2022; Sahu et al., 2023). There are numerous varieties of hydrological models, varying in complexity and specific application. These include the curve number (CN) conceptual rainfall-runoff model, which is used to estimate runoff based on vegetation cover and soil type (Verma et al., 2022; Forootan, 2023). Linear reservoir physical models represent a watershed using a single reservoir with inputs (precipitation) and outputs (flow) (Nourani et al., 2009). Monte Carlo simulation models estimate flood probabilities based on precipitation variability (Rahman et al., 2002; Loveridge and Rahman, 2018). Coupled hydrological models integrated with water quality models assess the impact of pollutant discharges on stream water quality. The soil and water assessment tool (SWAT), a physically-based distributed model (Neitsch et al., 2011), divides a watershed into multiple sub-basins, considering the unique characteristics of each sub-basin, enabling more detailed modeling of spatial variability in the hydrological system within a watershed (Yang et al., 2016; Worqlul et al., 2018).

The choice to utilize the SWAT model by researchers and decision-makers is currently driven by its ability to assess the hydrological system and sediment yield within a watershed (Francesconi et al., 2016; de Oliveira Serrão et al., 2022). It integrates various hydrological processes, accounts for agricultural management practices, and models the spatial variability of watershed characteristics (Krysanova and White, 2015; Briak et al., 2019). Moreover, SWAT allows for water quality modeling in addition to erosion, making it a versatile tool for watershed studies (Zettam et al., 2022). Its validation and calibration using SWAT-CUP, based on accurate measurements of flow rates and sediment concentrations at hydrometric stations, enhances the accuracy of the results by adjusting the model to the specific conditions of the study watershed (Chiang et al., 2023; Oduor et al., 2023). Consequently, SWAT is widely employed in hydrology research and water resource management, offering a robust approach to studying erosion and sedimentation, particularly in complex agricultural and environmental contexts.

Applying the SWAT model in Morocco presents significant challenges due to several factors. Firstly, the number of studies utilizing SWAT in the country is minimal. This limitation can be partly attributed to data availability constraints and the complexity of model application (Briak

et al., 2016; Ouallali et al., 2020). Secondly, Morocco needs more meteorological and hydro-metric stations, which constrain the amount and quality of data required for calibrating and validating the model. Furthermore, available data for these processes, including flow rates, sediment concentrations, and water quality data, are often scarce and sometimes cover only a short period, further complicating model validation over an extended timeframe.

Furthermore, the absence of detailed soil maps and precise pedological data, such as bulk density, pH, hydraulic conductivity, particle size distribution, and organic matter, for most Moroccan areas poses a significant challenge for model parameterization. The accuracy of these data is crucial for obtaining reliable results in hydrological simulations. Lastly, applying SWAT requires in-depth expertise and mastery of the tool, which can hinder model implementation (Halbe et al., 2018; Bodrud-Doza et al., 2023). Despite these challenges, SWAT is a valuable tool for evaluating and managing a nation's water resources, which face significant hydrological issues (Samimi et al., 2020; Jeyrani et al., 2021), underscoring the need to invest in data collection and training to enhance the model's application in the Moroccan context.

The present study presents an exceptional opportunity to address the challenges and issues associated with applying the SWAT model in Morocco. As an ideal and fundamental case study, it offers several crucial advantages for future SWAT applications in the country. Firstly, our study benefits from the availability of high-resolution land use and topographic data, an essential resource for accurate model parameterization. These detailed data provide a more accurate representation of watershed characteristics and contribute to more precise modeling of hydrological and erosion processes. Furthermore, we have access to detailed pedological data based on a comprehensive analysis of physicochemical parameters in soil profiles. This wealth of pedological data enhances the accuracy of modeling erosion and sedimentation processes. Additionally, the selected study area provides an ideal case regarding the size and spatial variability of erosion parameters, allowing us to obtain representative and generalizable results for other regions in Morocco.

Another significant advantage is the presence of a downstream reservoir in the study area, ensuring the supply of irrigation water, drinking

water, and hydroelectric power production. This characteristic makes the studied site important for regional water resource planning and management. Moreover, we have a historical dataset spanning 40 years, including daily and monthly data on flow rates, sediment concentrations, and precipitation. These extensive and detailed time series provide a solid foundation for model calibration and validation, thus enhancing the reliability of our study's results.

The objectives of this study are as follows: (i) Modeling soil erosion and sedimentation processes in the watershed using the SWAT model based on high-resolution land use and topographic data. (ii) Examine the spatial variability of erosion and sedimentation parameters in the study area and identify erosion-sensitive zones. (iii) Calibration and validation of the SWAT model using 40 years of historical data on flow rates and sediment concentrations to ensure the reliability of the modeling results. (iv) Evaluate the impact of erosion on the region's water resources, particularly on the downstream reservoir, by determining its sedimentation rate. (v) Recommend sustainable water resource management and soil conservation practices in the region based on study results and tested management scenarios. Thus, this study offers a reference model for sustainable water resource management in the region and contributes to addressing the hydrological challenges facing Morocco.

MATERIALS AND METHODS

Study area

The Oued El Makhazine dam, located approximately 10 kilometers southeast of Ksar El Kebir, controls a watershed with a surface area of 1.820 km². With its reservoir having a volume of 773 Mm³, it regulates average annual water inflows of 800 Mm³ at the site. Precipitation in this basin, primarily influenced by its proximity to the Atlantic Ocean, averages around 725 mm, resulting in a discharge of 1.200 Mm³ measured at the basin's mouth (Figure 1). The El Makhazine dam provides security and protection to the cities of Ksar El Kebir and Larache and the downstream plain through a significant reduction in flood events. The thirty-year flood flow has been substantially reduced from 4000 m³/s to 2000 m³/s. Additionally, this structure ensures a guaranteed

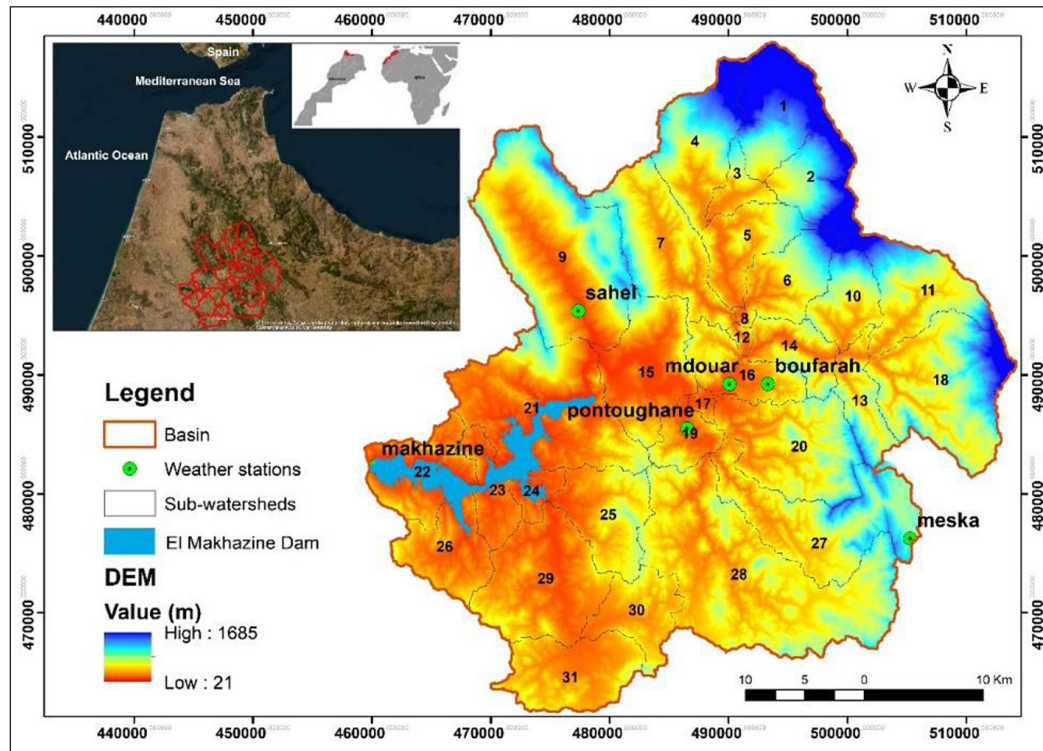


Figure 1. Geographical location of the study area (the numbers from 1 to 31 represent the sub-basins)

annual supply of 20 Mm³ of drinking and industrial water for the region. Most importantly, it facilitates irrigation across 35,000 ha within the Loukkos perimeter, delivering an annual volume of 270 Mm³ agricultural water.

Implementation of the model SWAT

The SWAT model offers flexibility in its operational scales, encompassing sub-daily, daily, monthly, and annual temporal resolutions. Within the framework of this investigation, ArcSWAT-2012, an integrated component of ArcGIS 10.3, facilitates the execution of the hydrological model. This interface utilizes key input data, including soil qualities, land-use patterns, topographical information, and climatic databases. Notably, the SWAT model can generate missing climatic parameters, such as humidity, solar radiation, and wind speed (Mengistu et al., 2019; Sharma et al., 2022).

The assessment of hydrological processes encompasses a diverse array of components, spanning infiltration, surface runoff, percolation, evaporation, evapotranspiration, as well as lateral and subsurface fluxes (Vereecken et al., 2022). Authoritative references, such as the SWAT manual and the comprehensive research conducted by Abbaspour et al., (2015), offer profound insights

into the requisite procedures for implementing the SWAT paradigm.

The SWAT model simulates the hydrological cycle and the water balance within the watershed using the formula (Equation 1).

$$SW_t = SW_0 \cdot \sum_{n=1}^t \left(\begin{array}{c} R_{day} - Q_{surf} - \\ - E_a - W_{seep} - Q_{gw} \end{array} \right) \quad (1)$$

where: W_{seep} is the amount of percolation and outflow from the bottom of the soil profile on day n (mm H₂O), W_{seep} is the amount of backflow on day n (mm H₂O), E_a is the amount of evapotranspiration on day n (mm H₂O), Q_{surf} is the quantity of surface runoff on day n (mm H₂O), and Q_{gw} is the quantity of backflow on day n (mm H₂O).

Using the modified soil loss equation (MUSLE) variables (Equation 2) (Williams, 1975; Talebizadeh et al., 2010), the SWAT model can additionally estimate the amount of sediment discharged at the watershed outlet and predict the sediment patterns:

$$Sed = 11.8 \cdot (Q_{surf} \cdot q_{peak} \cdot area_{hru})^{0.5} \cdot K_{usle} \cdot C_{usle} \cdot P_{usle} \cdot LS_{usle} \cdot F_{CFRG} \quad (2)$$

Sed represents soil loss in metric tonnes, Q_{surf} denotes surface runoff volume in $\text{mmH}_2\text{O/ha}$, q_{peak} signifies peak flow rate in m^3/s , and area_{hru} represents the area of Hydrological Response Units (HRUs) in hectares. Additionally, K_{USLE} , C_{USLE} , P_{USLE} , and LS_{USLE} represent the soil erodibility factors in units of $0.013 \text{ tonne m}^2 \text{ h} / (\text{m}^3\text{-metric tonne cm})$, the vegetation cover factor, erosion control practice factor, and topography factor, respectively. The final factor is the coarse fragmentation factor, CFRG.

The SWAT model was initially implemented in the watershed under study before calibration and validation. After these preliminary procedures, the model was used for simulating Best Management Practices (BMPs). The model employs fine-grained spatial and temporal units, with HRUs serving as the geographic resolution, adopting a daily time step. These units are characterized by homogeneity in terms of water, pedoclimate, and land use, as expounded by Gassman et al. (2007). While Hydrological Response Units are distributed across their respective sub-basins, they are not spatially distributed. These sub-basins, in turn, create stream segments that divide the catchment area. Calculations in the model are carried out at the scale of these units, utilizing various equations derived

from multiple studies (Neitsch et al., 2011). The model sequentially computes each variable based on available data.

In this study, we employed the SWAT model to assess various combinations of agricultural BMPs and source reduction strategies, investigating methods for reducing sediment loads within the basin. The assessment of model performance involved the application of statistical techniques to quantify the comprehensive soil erosion rate within the research area, as indicated by Briak et al. (2016). The model underwent calibration and validation processes, both of which were executed utilizing observed data.

Input datasets

Land use

The land use and land cover (LULC) data for this study were obtained from a recent high-resolution Sentinel-2 satellite image (10 m resolution) (<https://scihub.copernicus.eu/>), which was used to identify several landuse groups. The selection of an appropriate satellite image was guided by evaluating cloud cover patterns over the Oued El Makhazine basin during recent time frames. This criterion led to the identification of May 16, 2022,

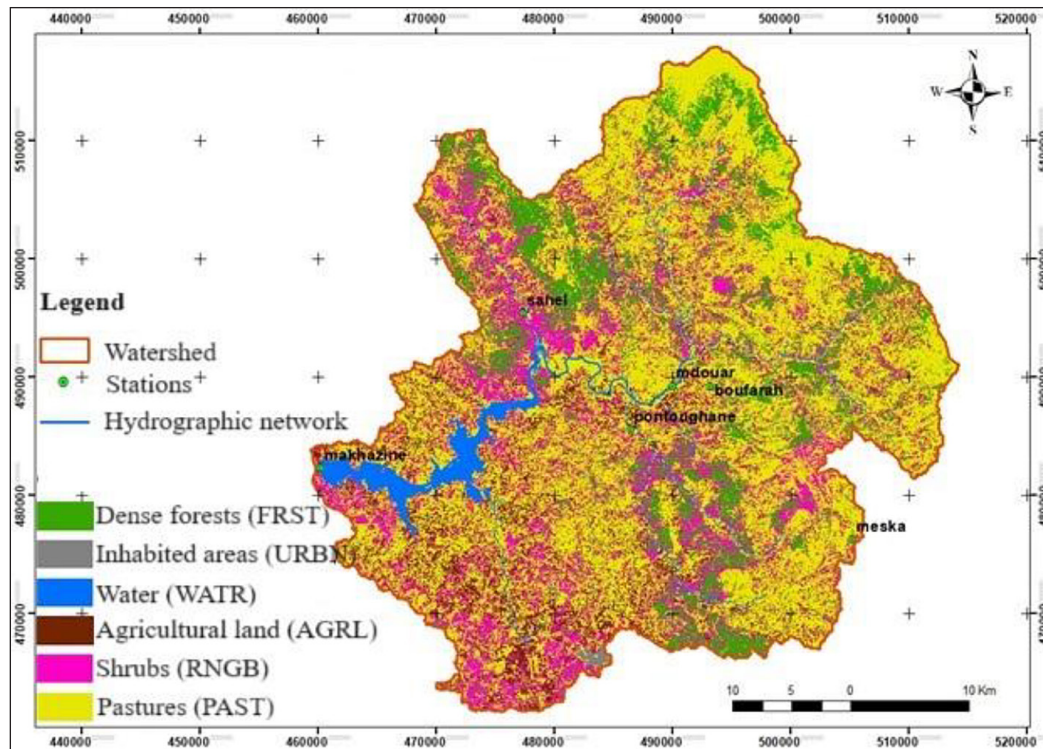


Figure 2. Land use and land cover map of the study area

as the optimal date for land use classification. Creating the land cover map for the study area was accomplished through an interactive supervised classification approach, which involved selecting regions of interest to enhance the precision of the obtained outcomes. Indeed, Google Earth Engine (GEE) was used to carry out the LULC classification utilizing the Random Forest (RF) algorithm. 350 Regions of Interest (ROIs) were created using field surveys, high-resolution base-maps, and visual interpretation to define training samples for six classes (forest, agriculture, urban, water, inhabited areas, bare soil, and pastures, for example). The RF classifier (100 trees) utilized the NDVI and the 10 spectral bands of Sentinel-2. A confusion matrix was created by using 250 stratified random validation points to evaluate accuracy after classification. Among the statistical metrics were class-specific user's accuracy (UA) and producer's accuracy (PA), Kappa coefficient (κ : 0.89), and Overall Accuracy (OA: 92%). The technique relies on supervised learning, in which the RF model is trained using spectral signatures from ROIs to generalize pixel-wise classifications throughout the basin, while reducing overfitting through the use of ensemble decision trees. The

distribution of the various LULCs in the basin studied is summarized in Figure 2.

Soil data

Soil type plays a crucial role in influencing both the magnitude and velocity of floods, as well as their specific erosive potential. Key factors, such as infiltration rates, moisture content, retention capacity, initial losses, and runoff coefficients, are all influenced, at least in part, by the characteristics of the soil type and its thickness. Soil data are extracted from the soil map (10 m resolution) of the study area prepared as part of a soil study carried out in the area in 2017 by NIAR (National Institute for Agronomic Research) (Belasri et al., 2017). Based on the soil map of the Oued El Makhazine watershed, the predominant soil types within the watershed include undeveloped soils and burnished soils, collectively covering 56% of the watershed's total surface area. Raw mineral soils, burnished soils, and fersiallitic soils represent another significant portion, accounting for 27% of the watershed's surface area. Lastly, vertisols and calcimagnesian soils encompass 17% of the watershed's surface area, as illustrated in Figure 3.

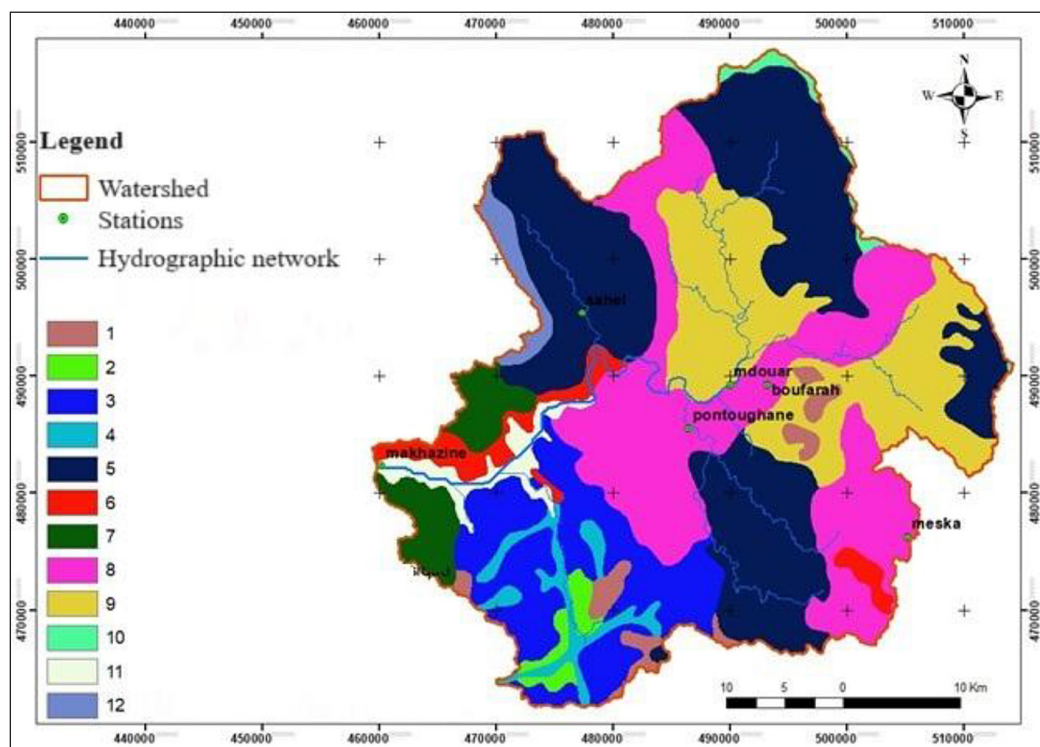


Figure 3. Soil map of the study area (Belasri et al., 2017). 1: Ferralitic soils, 2: Vertisols, 3: Calcimagnesian soils, 4: Undeveloped soils, 5: Poorly developed brown soils, 6: Soils with raw minerals, 7: Vertisols and calcimagnesian soils, 8: Complex soils (Poorly developed brown soils- calcimagnesian soils), 9: Undeveloped soils with raw minerals, 10: Brown soils with raw minerals, 11: Dam, 12: Brown soils with raw minerals-ferralitic soils)

Topographic data

Understanding the topographical characteristics is pivotal in elucidating the hydrological dynamics of the watershed. Figure 1 above provides a visual representation of the digital elevation model employed to illustrate the topographical features and elevation profiles within the Oued El Makhazine watershed. The relief map utilized in this study is derived from the digital terrain model (ALOS PALSAR) and topographic maps encompassing the study area. The elevation map reveals a range of altitudes spanning from 21 to 1681 meters between the lowest point, where the dam is situated, and the hilly terrain. The higher elevations are predominantly located upstream in the basin, generally to the north and northeast, whereas the lower-lying areas are in proximity to the dam site (Figure 1). Regarding slope characteristics, Figure 4 illustrates the spatial distribution of slopes within the basin. This map was generated using the ArcGIS slope tool, with a Digital Terrain Model serving as the reference. The obtained slope values were categorized into five classes, typically spanning from $< 5\%$ to $> 45\%$. The highest slope values are primarily concentrated in the central and eastern regions of the basin, with the upstream

zone also displaying varying degrees of steepness across different locations.

ArcSWAT-2012 utilizes topographic data derived from a digital terrain model, as illustrated in Figure 1, to calculate stream directions, slopes, and accumulations. Leveraging this information and the identification of outlets, the automatic delineation of sub-basins is achieved. Soil maps, slope data, and land use information facilitate the definition of the watershed through the establishment of Hydrologic Response Units (HRUs) by the SWAT model.

ArcSWAT-2012 also possesses the capability to generate data tables for all HRUs, watershed units, and watercourses. Furthermore, it can determine parameter values within the hydrological cycle based on input data and time dependencies. Consequently, modeling data encompassing sediment generation, water discharge, evaporation, evapotranspiration, fluxes, percolation, as well as simulated flows and sediment deposition are computed. For an accurate representation of real-basin conditions, data calibration and validation are imperative. In this context, the SWAT Calibration and Uncertainty Processors were selected due to their availability for calibrating and validating the simulated outputs of ArcSWAT-2012.

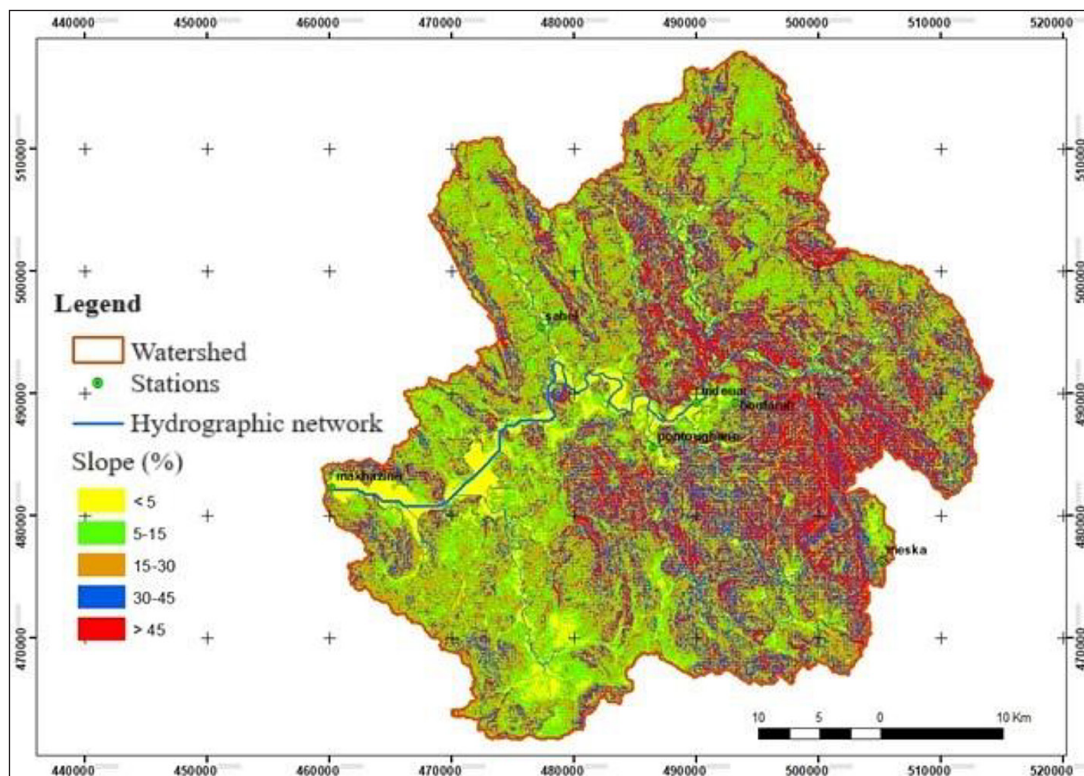


Figure 4. Slope map of the study area

Swat-cup

Linking to the SWAT-CUP model, a software tool primarily designed for data calibration, validation, and sensitivity analysis within the SWAT model (Abbaspour et al., 2007), has been employed in this study. It utilizes the output data files generated by SWAT, specifically in the TxtInOut format, to enhance the dependability of results by incorporating various parameters that influence the water cycle, such as CN2, Sol_AWC, SOL_K, and other relevant factors. The application of the Sufi-2 methodology involved calibrating, validating, and conducting sensitivity analyses of simulated flows and sediment outputs in comparison to observed values. Utilizing the Sufi-2 algorithm, the estimation of measurement uncertainty (for both flow and sediment) was performed within the 95% prediction uncertainty (95PPU) framework of the SWAT-CUP software (Abbaspour et al., 2015). This estimation considered sensitivity parameters used during model calibration, each defined by pre-determined minimum and maximum ranges.

Abbaspour et al. (2015) introduced two metrics to assess the precision of model uncertainty calibration. The initial metric, denoted as P, expresses the percentage of measured data (inclusive of errors) that fall within the 0-1 interval of the 95% prediction interval (PPU), with 1-P representing model error (Abbaspour et al., 2004). The second metric, denoted as R, represents the ratio of the standard deviation of the measurement to the width of the 95% probability of prediction (PPU) band (Abbaspour et al., 2015). This parameter, ideally below 1.5, functions as an indicator for model calibration and validation.

In the context of Sufi-2, the user has the flexibility to choose from eleven objective functions extracted from the observed.txt file, and this selection significantly impacts the available calibration solutions. The choice is often aligned with the specific objectives of the study. The model's fitness was assessed using the Nash-Sutcliffe model efficiency coefficient (NSE) (Equation 4), the percent bias (PBIAS) (Equation 5), and the coefficient of determination (R^2) (Equation 3).

$$R^2 = \frac{(\sum_{i=1}^n (Q_{si} - Q_s) \cdot (Q_{mi} - Q_m))^2}{\sum_{i=1}^n (Q_{si} - Q_s)^2 \cdot \sum_{i=1}^n (Q_{mi} - Q_m)^2} \quad (3)$$

In the context of the given expression, where in Q_{mi} denotes the observed value, Q_{si} represents the simulated value, Q_m is the mean of the observed values, and Q_s is the mean of the simulated

values, the coefficient of determination, denoted as R^2 , is employed as a statistical measure.

$$NSE = 1 - \frac{\sum_{i=1}^n (Y_i^{obs} - Y_i^{sim})^2}{\sum_{i=1}^n (Y_i^{obs} - Y_{mean})^2} \quad (4)$$

$$PBIAS = \frac{\sum_{i=1}^n (Y_i^{obs} - Y_i^{sim}) \cdot 100}{\sum_{i=1}^n Y_i^{obs}} \quad (5)$$

In the presented context, Y^{sim} signifies the predicted stream flow (m^3/s) at time t , while Y^{obs} represents the observed stream flow (m^3/s) at the same time instance.

Model sensitivity parameters

The monthly streamflow and sediment load data used for model calibration and validation were obtained from four primary gauge stations located within the study watershed (Sahel, Mdouar, Oughane, and Makhazine stations). Data availability for these stations spanned from 1979 to 2019, based on records provided by the National Water Resources Authority. Before model application, all datasets underwent quality control procedures to detect and correct inconsistencies or missing values. To ensure model stability and reliability, the simulation period was divided into three distinct phases: a warm-up period (1979–1981), a calibration period (1982–2002), and a validation period (2003–2019). These intervals were uniformly applied across all selected stations to allow for consistent performance comparison and robust uncertainty analysis.

A global sensitivity analysis was conducted using the Sequential Uncertainty Fitting version 2 (SUFI-2) algorithm embedded in the SWAT-CUP software package (Abbaspour, 2011). Key parameters influencing simulated flow and sediment outputs were identified and categorized according to their dominant effects: those affecting hydrological processes (e.g., CN2, GW_DELAY) and those influencing erosion and sediment transport (e.g., USLE_K, SED_EXPO_CO1). Parameter bounds were initially defined based on SWAT-CUP guidelines and refined iteratively through successive simulations (Tables 1 and 2) (Yang et al., 2008).

A total of 1500 iterations were executed to explore the parameter space and reduce predictive uncertainty. Model convergence was observed after approximately 400 iterations, as indicated by stable values of the Nash–Sutcliffe Efficiency (NSE) and Percent Bias (PBIAS). Following established performance thresholds, simulations

Table 1. Sensitivity parameters used for flow calibration and validation

Parameter	Definition	Min	Max
R_CN2.mgt	Runoff curve number	-0.2	0.2
R_SOL_AWC().sol	Available water capacity of the soil layer in question (mm H2O/mm soil)	-0.25	0.25
R_SOL_BD().sol	Wet bulk density	-0.5	0.6
R_SOL_K().sol	Saturated hydraulic conductivity	-0.25	0.25
V_GWQMN.gw	Minimum water depth for water transfer from shallow aquifer to stream, from shallow aquifer to watercourse	0	2
V_REVAPMN.gw	Maximum water threshold in shallow aquifer for revap to occur (mm)	0	500
V_ESCO.hru	Soil evaporation compensation factor	0.01	1
V_SURLAG.bsn	Response time due to surface runoff	0.5	10
V_GW_DELAY.gw	Time taken for groundwater transiting the shallow aquifer to reach the watercourse (days)	30	450
V_ALPHA_BF.gw	Groundwater base flow recession constant	0	1
V_CH_N2.rte	Manning's coefficient "n" of the main channel	0	0.3
v_GW_REVAP.gw	Coefficient allowing the transfer of water from the aquifer to the overlying, unsaturated soil horizons.	0	0.2
v_CH_K2.rte	Effective hydraulic conductivity in main watercourses	5	130
r_SLSUBBSN.hru	Average sub-basin slope length	0	0.2
v_SURLAG.bsn	Response time due to surface runoff	0.5	10
r_HRU_SLP.hru	Average slope steepness (m/m)	0	0.2
r_OV_N.hru	Manning's "n" value for overland (kg/ha)	-0.2	0
v_ALPHA_BNK.rte	Baseflow alpha factor for bank storage (days)	0	1

Table 2. Sensitivity parameters used for sediment calibration and validation

Paramètre	Définition	Min	Max
v_ADJ_PKR.bsn	Peak flow adjustment factor for sediment conveyance in the subbasin (tributary channels)	0.5	2
v_CH_COV1.rte	Channel erodibility factor	-0.05	0.6
r_USLE_K().sol	Soil erodibility factor (0.013 t.m ² .h/m ³ .t.cm)	0	0.65
v_SPCON.bsn	Linear parameter for calculating the maximum amount of sediment that can be entrained during channel transport	0.0001	0.01
v_SPEXP.bsn	Exponent parameter for calculating reentrained sediments in channel sediment transport	1	1.5
v_USLE_P.mgt	Conservation practice factor	0	1
v_CH_COV2.rte	Facteur de couverture végétale du canal	-0.001	1

were deemed acceptable when the NSE exceeded 0.5 and the PBIAS remained below $\pm 25\%$ during both the calibration and validation phases (Ghoraba, 2015; Halecki et al., 2018). These criteria ensured that model predictions were both statistically reliable and practically helpful for decision-making in watershed management contexts.

Best management practices (BMPs)

Our primary emphasis was on evaluating how the SWAT model captured the representation of four practical land management practices: contouring, strip cropping, terracing, and

reforestation. Contouring applied to a field, through the retention of water in small depressions, achieves the following outcomes: (1) diminishes surface runoff, (2) mitigates sheet and gully erosion by reducing the erosive force of surface runoff and averting or minimizing channel development. Strip-cropping diminishes surface runoff by retaining water in small depressions, imparts surface roughness to decelerate runoff, and curtails sheet and gully erosion by obstructing channel formation. Implementation of terracing in a field results in (1) a reduction in peak flow rate due to shorter slopes, (2) a decline in surface runoff by retaining water in depressions,

and (3) diminished sheet and gully erosion by enhancing sediment settling in runoff, diminishing its erosive potential, and preventing the formation of rills and gullies. The implementation of Best Management Practices (BMPs) was based on adjusting two pivotal parameters. The initial parameter, the curve number (CN), plays a crucial role in calibrating the hydrological components of the SWAT model. The second component involves the USLE Support Practice Factor (USLE_P). The modifications to these parameters were informed by previous research and modeling endeavors conducted in watersheds, as detailed in Neitsch et al. (2005) and Arabi et al. (2008).

RESULTS

Analyzing model sensitivity

The watershed was divided into 31 subwatersheds and 425 hydrologic response units (HRUs) using ArcSWAT software, with flow and sediment measurements taken at hydrometric stations in subwatersheds 9, 16, 19, and 22. Tables 3 and 4 present the optimal values for 23 parameters used in the calibration and validation of flow and sediment content over a 41-year period. For example, a significant response of an outcome measure indicates that it is very sensitive to the output

results (Guzman et al., 2015). When we consider a parameter to be sensitive, its p-value approaches 0, and we find that 23 parameters exhibit the highest sensitivity within our study area. These parameters include CN2.mgt, ALPHA_BF.gw, GW_DELAY.gw, GWQMN.gw, GW_REVAP.gw, ESCO.hru, CH_N2.rte, CH_K2.rte, ALPHA_BNK.rte, SOL_AWC(..).sol, SOL_K(..).sol, SOL_BD(..).sol, SFTMP.bsn, HRU_SLP.hru, OV_N.hru, SLSUBBSN.hru for flow parameters, and CH_COV1.rte, ADJ_PKR.bsn, CH_COV2.rte, USLE_P.mgt, SPEXP.bsn, SPCON.bsn, USLE_K(..).sol for the sediment patterns.

In our study region, we have identified critical determinants with high sensitivity, including Manning's coefficient 'n' for the main channel CH_N2 and SOL_K. These parameters result in increased water infiltration from surface water and soil runoff. Additionally, we consider the GWQMN parameter, which influences the quantity of water passing through the soil and, consequently, runoff, as a key component in our research.

When it comes to controlling sediment transport in the basin's channels and streams, SPCON stands out as the most sensitive parameter, set at 0.004 (Li et al., 2021). Furthermore, SPEXP exhibits significantly higher sensitivity than USLE_P, prompting us to adjust its value to 0.947 to calculate redistributed sediments in channel sediment conveyance. Both USLE_P and SPEXP

Table 3. Sensitivity parameters used for flow simulation and their calibrated values

Parameter names	Rank	Min_value	Max_value	Final value	t-statistic	P-Value
R_CN2.mgt	1	-0.020	0.044	-0.009	-0.353	0.72
V_ALPHA_BF.gw	2	0.541	0.775	0.759	0.687	0.49
V_GW_DELAY.gw	3	382.764	520.392	465.203	0.410	0.68
V_GWQMN.gw	4	2.075	2.436	2.363	0.994	0.32
V_GW_REVAP.gw	5	-0.047	0.008	-0.035	-0.069	0.95
V_ESCO.hru	6	0.681	0.761	0.713	0.038	0.97
V_CH_N2.rte	7	-0.084	0.141	-0.040	14.865	0.00
V_CH_K2.rte	8	-78.418	-38.005	-56.958	0.277	0.78
V_ALPHA_BNK.rte	9	0.871	0.987	0.891	-0.717	0.47
R_SOL_AWC(..).sol	10	0.083	0.304	0.251	-0.275	0.78
R_SOL_K(..).sol	11	-1.149	-0.638	-0.954	1.927	0.05
R_SOL_BD(..).sol	12	-0.098	0.088	-0.014	0.147	0.88
V_SFTMP.bsn	13	11.241	15.142	15.106	0.250	0.80
R_HRU_SLP.hru	14	0.101	0.133	0.120	-0.610	0.54
R_OV_N.hru	15	-0.055	-0.019	-0.026	1.244	0.21
R_SLSUBBSN.hru	16	0.056	0.105	0.091	-0.128	0.90

Note: V: means the existing parameter value is to be replaced by a given value; R: means an existing parameter value is multiplied by (1 + a given value).

Table 4. Sensitivity parameters used for sediment simulation and their calibrated values

Parameter names	Rank	Min_value	Max_value	Final value	t-statistic	P-value
V__CH_COV1.rte	17	0.380	0.716	0.495	0.716	0.47
V__ADJ_PKR.bsn	18	-0.289	2.571	1.435	-0.485	0.63
V__CH_COV2.rte	19	0.081	0.780	0.762	0.984	0.33
V__USLE_P.mgt	20	0.957	2.147	1.296	0.862	0.39
V__SPEXP.bsn	21	0.816	1.126	0.947	-2.161	0.03
V__SPCON.bsn	22	0.003	0.014	0.004	-11.831	0.00
R__USLE_K(..).sol	23	-0.062	0.345	0.283	-1.385	0.17

Note: V: means the existing parameter value is to be replaced by a given value; R: means an existing parameter value is multiplied by (1 + a given value).

parameters impact sediment movement within channels and streams (Li et al., 2021) and have implications for soil treatment practices within the watershed.

Calibrating, validating, and performance model analysis

According to several authors, adopting a multi-objective and multi-variable calibration approach is preferable over a mono-objective strategy (Wang et al., 2019). In our study, we consider three objective functions to assess model performance. These functions quantify the model's efficiency by measuring the correlation between the variability in observed data and the accuracy of the model's fit (Duru et al., 2018). When the NSE is greater than 0.50, the PBIAS for streamflow is within $\pm 25\%$, and the PBIAS for sediment is within $\pm 55\%$, the

model simulation is considered adequate (Moriassi et al., 2007). The best results from multi-objective optimization during both calibration and validation are summarized in Table 5. The NSE, PBIAS, and R² values obtained demonstrate a favorable alignment between observed and simulated data, indicating a satisfactory model performance. Notably, R² exhibits high values during both periods. While flow rates increase when transitioning from the adjustment phase to the validation stage, sediment concentration shows only a slight decrease.

However, the hydrological cycle variables began to show meaningful and reasonable values after calibration based on the model's sensitivity parameters. Calibration attempts to correlate the model's response as accurately as possible with the empirical and observational data collected at the hydrological gauging station.

Table 5. Results of the multi-objective optimization for the calibration and validation period (NSE, R², and PBIAS) (Sediment concentration values are only available for the El Makhazine station; NA means not applied)

Stations	Parameters	Calibration period		Validation period	
		Flows	Sediments	Flows	Sediments
Sahel (sb-9)	NSE	0.70	NA	0.62	NA
	R ²	0.72	NA	0.63	NA
	Pbias	-7.15	NA	1.53	NA
Mdouar (sb-16)	NSE	0.64	NA	0.44	NA
	R ²	0.70	NA	0.50	NA
	Pbias	19.99	NA	-21.63	NA
Oughane (sb-19)	NSE	0.58	NA	0.58	NA
	R ²	0.75	NA	0.63	NA
	Pbias	-66.84	NA	-37.48	NA
Makhazine (sb-22)	NSE	0.68	0.62	0.75	0.73
	R ²	0.73	0.62	0.78	0.78
	Pbias	-27	14	-25	2.56

Note: Sediment concentration monitoring within the El Makhazine watershed is limited to a single station at the outlet of sub-basin 22; thus, sediment data statistics are designated as 'not applicable' (NA) for all other sub-basins.

The outcomes of the multicriteria calibration for both flow and sediment, conducted through the Sufi-2 method within SWAT-CUP, are depicted in the Figures 5 and 6.

The data indicate that the calibration has been successful, as there are no significant differences between the observed and simulated variations in flow and sediment. This is particularly noteworthy given the relatively high correlation, as depicted in Figures 5 and 6. The performance of the model can be effectively assessed through sensitivity parameters when NSE, PBIAS, and R2 values are satisfactory, following the approach outlined by Uniyal et al. (2019). This framework is applicable in our case, as shown in Table 5, suggesting that the flow and sediment calibration procedure

aligns well with measurements and falls within acceptable limits.

The model underwent validation spanning an eight-year duration, from 1993 to 2000. Sufi-2 incorporates a distinctive iterative process comprising an equivalent number of simulations as observed during the calibration period (Rivas-Tabares et al., 2019). This iterative approach ensures the consistent replication of simulation outcomes over time by employing the same optimal sensitivity parameter ranges established during the calibration phase (Li et al., 2021). The model's performance throughout the validation period is assessed through the examination of objective function output results (NSE, PBIAS, and R2). The values obtained serve as

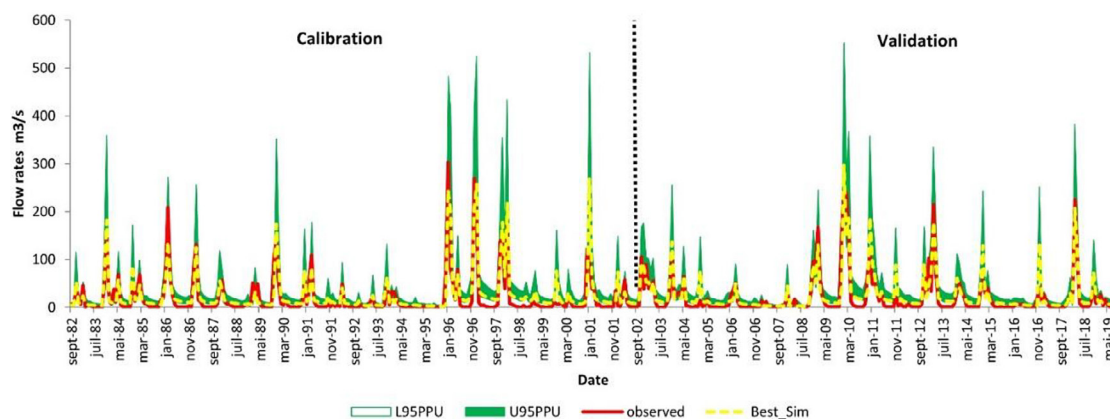


Figure 5. Observed and simulated flows (Stream Flow) for the calibration and validation periods (The L95PPU and U95PPU represent the lower and upper limits of the 95% prediction uncertainty interval for the model's predictions, and the Best_sim refers to the best simulation and the best model parameter set obtained after the calibration process)

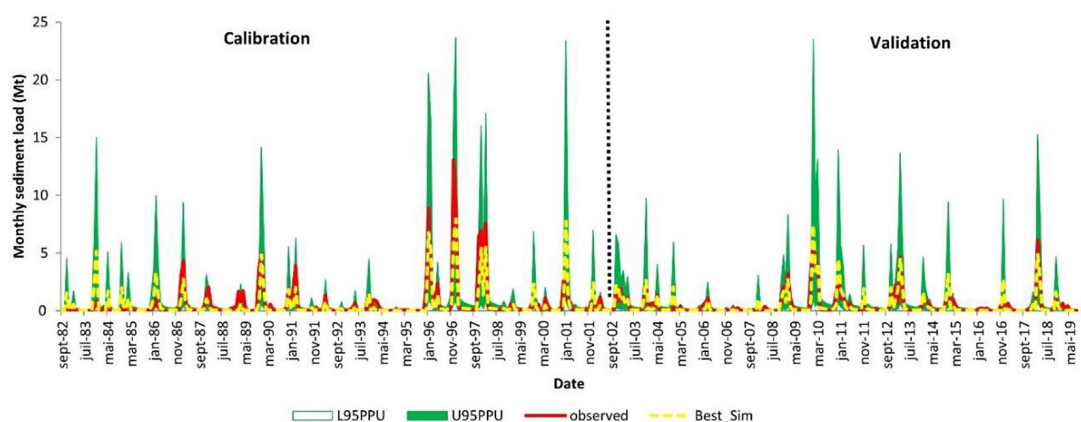


Figure 6. Observed and simulated sediment concentration for the calibration and validation periods (The L95PPU and U95PPU represent the lower and upper limits of the 95% prediction uncertainty interval for the model's predictions, and the Best_sim refers to the best simulation and the best model parameter set obtained after the calibration process)

indicators of successful model validation, as detailed in Table 5 and visually presented in Figures 7 and 8.

Water yield and water balance

SWAT analyses are conducted to evaluate the water balance and water yield, crucial parameters for the effective management of water resources within a given catchment area (Ayivi and Jha, 2018). Among the various components influencing the water balance, evapotranspiration emerges as the primary factor contributing to water loss in the catchment, surpassing surface runoff, as illustrated in Figure 9. Specifically, over the period from 1982 to 2019, evapotranspiration represents 52.17% of the simulated time, while surface runoff accounts for 27.71%. Notably, the remaining components of the water balance exhibit minimal fluctuations throughout the simulated timeframe. Consequently, within the Makhazine catchment, the dominant elements are identified as evapotranspiration (ET) and surface runoff. This

dominance is attributed to factors such as vegetation characteristics in the study area and elevated temperatures, particularly during the dry season.

The graphical representation in Figure 9 delineates the yearly mean of distinct water balance components in each sub-basin from 1982 to 2019, along with the cumulative annual average for the entire basin. Evapotranspiration and surface runoff jointly contribute to 79.88% of the entirety of water equilibrium components, while lateral flow and deep aquifer recharge collectively constitute only 4.20%. Owing to the absence of a deep aquifer in the region, losses due to water transmission and recharge to the deep aquifer remain below 2%. The spatial distribution of water balance elements within each sub-watershed is intricately influenced by factors such as land use type, soil characteristics, slope, and precipitation patterns.

Assessing water balance and yield is essential for understanding hydrological behavior in the Makhazine watershed and directly supports the study's goal of modeling watershed processes with SWAT. Identifying evapotranspiration and

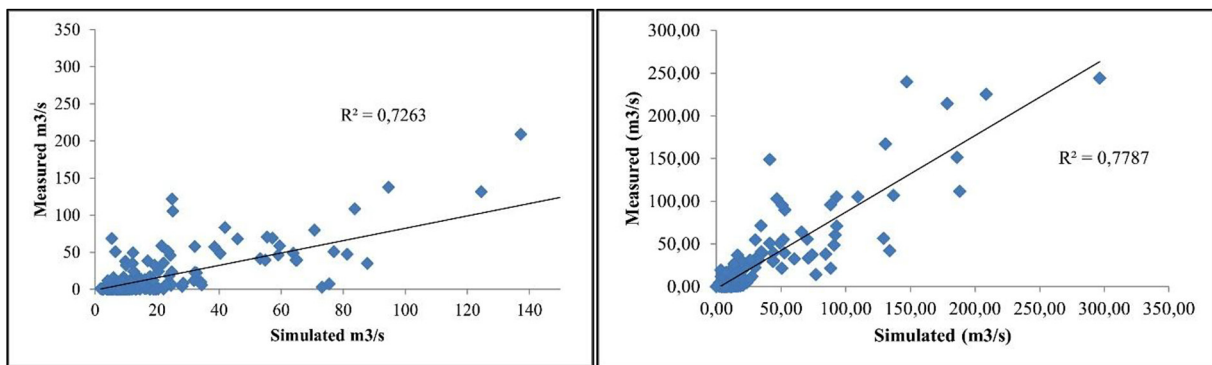


Figure 7. Scatter plot of observed and simulated monthly flows (StreamFlow) for the calibration & validation periods

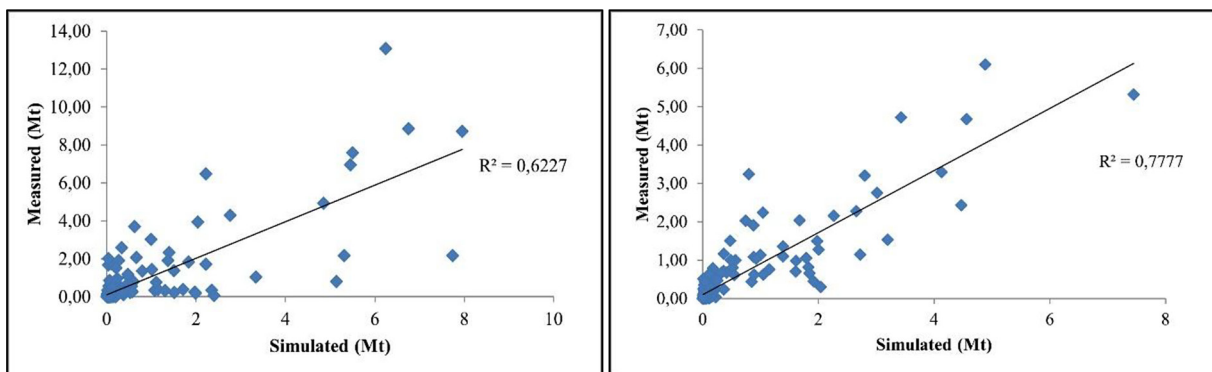


Figure 8. Scatter plot of observed and simulated monthly sediment concentrations for the calibration & validation periods

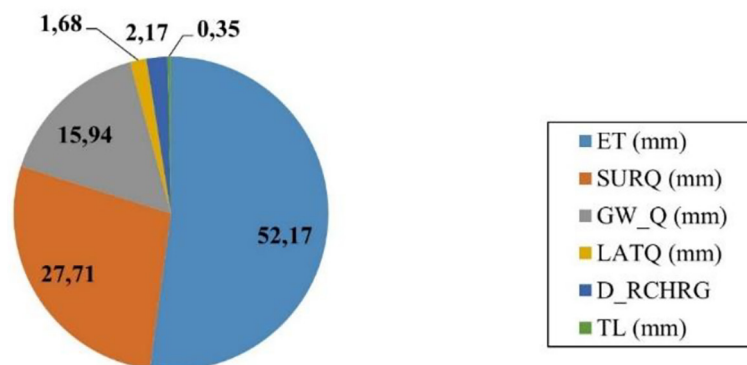


Figure 9. Water balance for the simulated period (1982–2019) expressed as a percentage compared to annual precipitation (ET: Evapotranspiration, SURQ: Surface runoff, GW_Q: Groundwater delay, LATQ: Lateral flow, TL: Transmission losses)

surface runoff as dominant components provides critical insights into water distribution and availability, which are essential for effective water resource management. The spatial variation of these components across sub-basins highlights the impact of land use, soil, and topography, underscoring the need for tailored conservation strategies. These findings also lay the groundwork for calibrating and validating the model, ensuring reliable simulations over the 41 years. Quantifying water yield ultimately contributes to the evaluation of the region's water resources and supports the development of sustainable management practices.

The SWAT model predicts water yield values ranging from 551.74 mm to 634.89 mm, with a

mean of 592.9 mm (Figure 10). The peak water yield is observed at sub-basin 27, in contrast to the minimum at sub-basin 23. Noteworthy is the concentration of higher values in the eastern and extreme north-western zones of the study area. At the same time, the central expanse of the watershed consistently presents moderate water yield values.

Sediment yield

Upon completion of the model calibration and validation phases employing precise sensitivity settings, SWAT-CUP generates text files containing monthly sediment yield values for

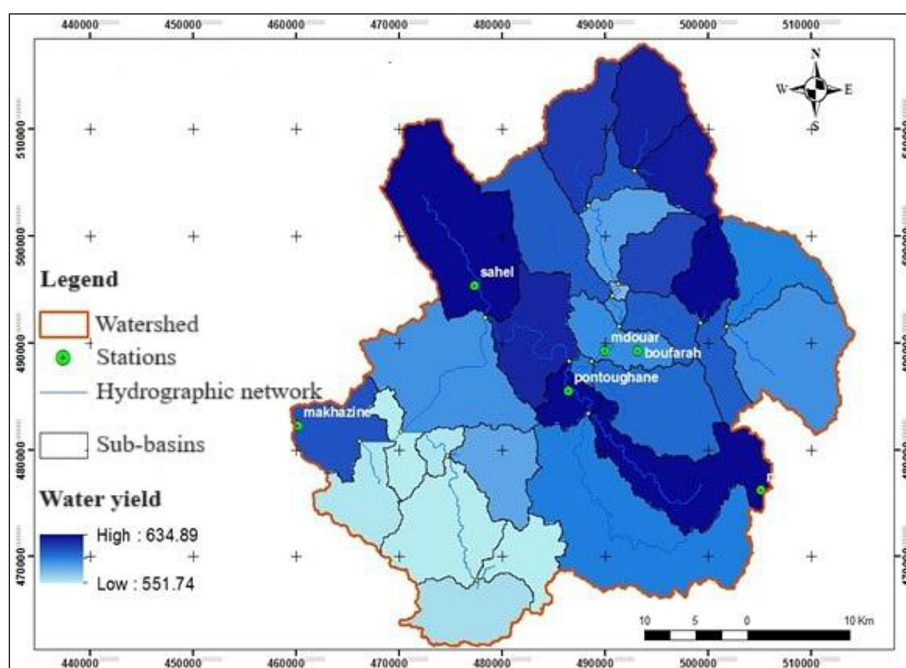


Figure 10. Water yield distribution map in each sub-watershed of the study area

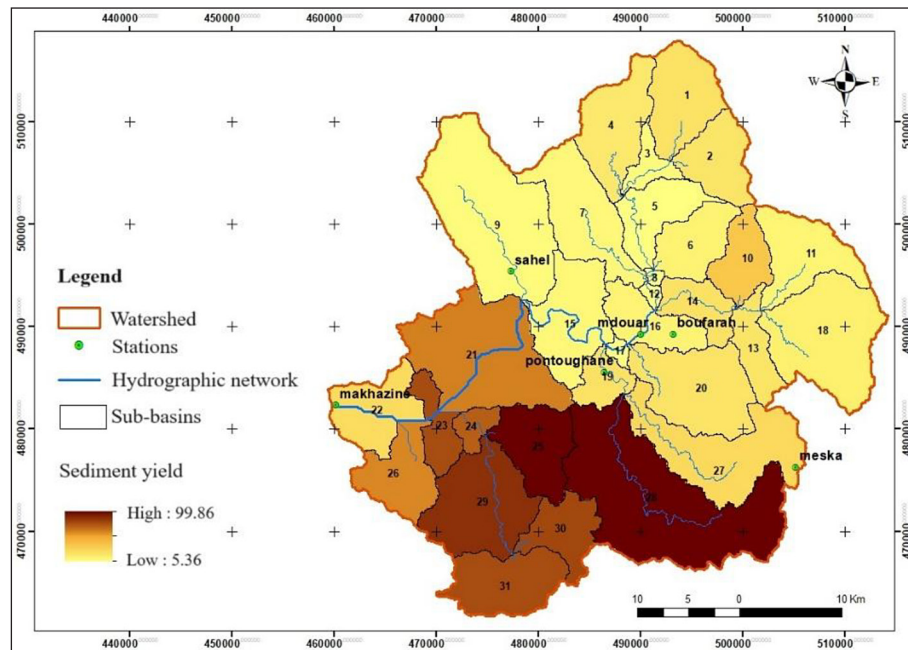


Figure 11. Distribution map of sediment yield values (t/ha/y) in the watershed

individual sub-basins. The anticipated sediment yields exhibit a spectrum, ranging from 5.36 t/ha/yr in sub-watershed 17 to 99.86 t/ha/yr in sub-watershed 25, with an average of 29.34 t/ha/yr (Figure 11). Depending on the state of the factors driving erosion, this figure shows the areas that produce the most sediment. The southern part of the basin is where more sediment is released, as it is mainly occupied by friable marl formations, which favor runoff, relatively high slopes, easily degradable

undeveloped soils, and degraded reworked croplands and/or pastures unprotected against erosion. The downstream part of the watershed generally releases less sediment and is less prone to erosion. Because of the state of the major erosion factors limiting the erosive process, these low losses also occur in the central part of the basin. Analysis of erosion rates over the years and across the various sub-watersheds has enabled us to identify the area most prone to erosion. Figure 12 illustrates the distribution

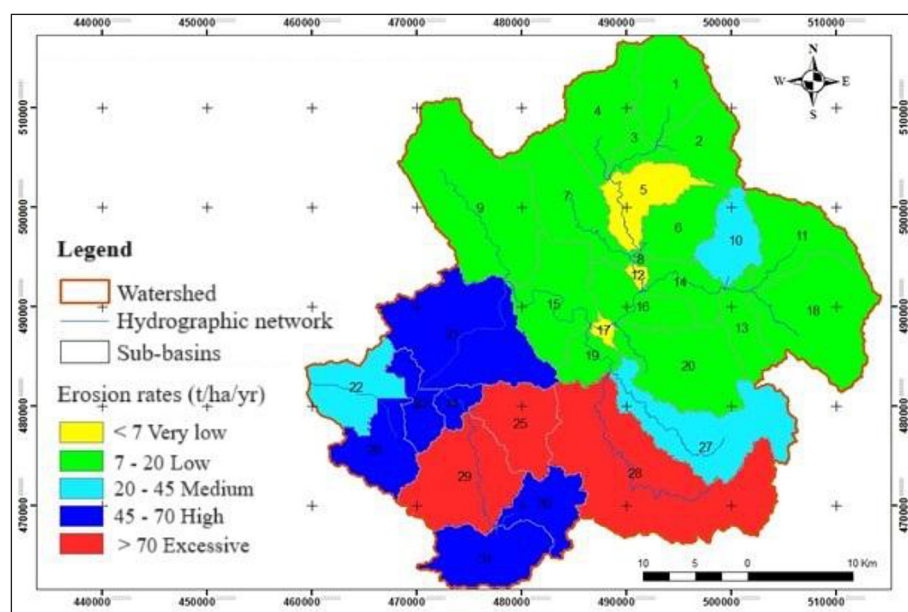


Figure 12. Map of erosion rates in the Oued Makhazine basin

of erosion rates and risks in the watershed. This map was created using a reclassification based on the classes most commonly used in scientific literature. An erosion rate of less than 7 t/ha/yr is generally considered very low and within acceptable limits, indicating stable soil conditions and minimal surface runoff (Ganasri and Ramesh, 2016). However, when erosion values exceed 20 t/ha/yr, they become alarming, often signaling accelerated soil loss that can degrade land productivity and water quality, particularly in agricultural or deforested areas (Abdulwahid et al., 2022; Talebizadeh et al., 2020). In general, the northern part of the basin is better protected against erosion due to its physical and chemical characteristics. By contrast, the southern part of the study area is the most vulnerable, with the highest erosion rates.

Table 6 presents an order of priority for anti-erosion intervention, where basins 25, 28, 29, 30, 31, 23, 24, 21, and 26 are identified as the primary sources of sediment, located mainly in the extreme south of the study area. These areas, which are at excessive risk of erosion, represent approximately 36.53% of the total watershed area, or more than a quarter. The center of the watershed (sub-basins 5, 8, 12, and 17) appears to be the most stable area in terms of erosion, showing low sediment production, representing 3.05% of the total watershed area. However, half of the study area (50.11%) falls within the average erosion class, with average rates ranging from 7 to 20 t/ha/yr (Table 6). By adopting the erosion rate classification most used in the scientific literature, where a rate exceeding 20 t/ha/yr indicates an alarming state of soil loss, suitable land management practices can be simulated for this area, particularly in basins 10, 21, 22, through to 31.

Best management practices (BMPs)

Estimation of the sediment yield of BMPs

The calibrated SWAT model was applied to compute soil loss, utilizing four distinct methodologies to assess erosion induced by various practices. Adjustments to the model's general parameters were made to accommodate the integration of four separate Best Management Practices (BMPs). The parameter modifications, elucidated in Arbi et al. (2008), were rooted in prior research and modeling endeavors conducted in watersheds with relevant data for sediment load calibration.

Assuming it is challenging to develop a watershed's entire area, BMP predictions were only applied to sub-watersheds in the El Makhazine watershed that had erosion rates exceeding 20 t/ha/year. The general parameters of the model were adjusted to account for the application of different agricultural BMPs. These changes to the parameters are based on previous research and modeling attempts on the watersheds. The primary parameters that need to be adjusted when implementing BMPs are the CN and USLE-P parameters. The parameters to be modified and incorporated into the SWAT model are shown in Table 7. The reduction in sediment production resulting from the use of these related practices was simulated using these values.

Subsequently, the SWAT model was deployed to calculate the annual average sediment loads for the El Makhazin watershed. The ensuing Table 8 delineates the anticipated quantities of eroded silt in each subwatershed after the implementation and simulation of agricultural best management practices. Recommendations for the identification and implementation of these best management practices have been proffered based on the study's findings.

Terracing

One of the most appropriate practices in the El Makhazine basin seems to be the implementation of terracing to reduce the effect of slope and runoff (Figure 13). The average rate of erosion

Table 6. Classification of sub-watersheds according to priority for anti-erosion intervention based on different soil erosion classes in the El Makhazine watershed

Erosion rate (t/ha/an)	Sub-watershed	Percentage (%)	Erosion class
0–7	5,8,12,17	3.05	Low
7–20	1,2,3,4,6,7,9,11,13,14,15,16,18,19,20	50.11	Medium
20–40	10,22,27	10.31	High
> 40	21,23,24,25,26,28,29,30,31	36.53	Excessive

Table 7. Evaluated BMPs, revised SWAT parameters, and adopted criteria for the Makhazine watershed

BMP type	BMP name	Adjusted parameter	Value	Adoption criteria	References
Structural practices	Terracing	TERR_SL (.ops)	$(0.1 \cdot \text{SLOPE} \cdot 0.9) \cdot 100 / \text{SLOPE}$	All subbasins/All landuse/All soils/All slopes	Neitsch et al., 2005 Arabi et al., 2008 Briak et al., 2019 Silva et al., 2024
		TERR_CN (.ops)	-6 (CN=68.52)		
		TERR_P (.ops)	0.11, for slope 0–5%; 0.12, for slope 5–15%; 0.16, for slope 15–30%, and 0.18 for slope > 30%		
	Contour farming	CONT_P(.ops)	0.55, for slope 0–5%; 0.57, for slope 5–15%; 0.8, for slope 15–30%, and 0.9 for slope >30%	All subbasins/All landuse/All soils/All slopes	Arabi et al., 2008 Briak et al., 2019 Silva et al., 2024
		CONT_CN(.ops)	-3 (CN=71.52)		
Vegetative measures	Strip cropping	STRIP_P(.ops)	0.27, for slope 0–5%; 0.29, for slope 5–15%; 0.4, for slope 15–30%, and 0.45 for slope > 30%	All subbasins/All landuse/All soils/All slopes	Arabi et al., 2008 Briak et al., 2019 Silva et al., 2024
		STRIP_CN(.ops)	-3 (CN=71.52)		
		STRIP_C(.ops) STRIP_N(.ops)	Adjusted based on the area weighted average values for the strips in the system (STRIP_C (0.4); STRIP_N (0.15))		
LULC Change	Reforestation	Change of the land use in the target HRUs	Reforestation of 30% in the target HRUs	Erosion > 20 t/ha Slope > 30%	Arnold et al., (2012) Ricci et al., 2020

has been reduced to a value of 10.32 t/ha/year, i.e. a reduction rate of about 64.8%, calculated using the following equation (Equation 6):

$$A(\%) = \frac{T_i - T_s}{T_i} \cdot 100 \quad (6)$$

where: (*A*) is the erosion reduction rate in percent, (*T_i*) is the average rate from the first simulation after calibrating the model in t/ha/yr, and (*T_s*) is the average rate in t/ha/yr after applying a BMP.

Strip-cropping

Strip cropping ranks second in terms of erosion reduction, with an average rate of 14.37 t/ha/year, a decrease of 51.02% (Figure 13). This technique also addresses the effect of slopes as a significant cause of erosion.

Contouring

By simulating crops planted parallel to the contour lines, the average erosion rate was reduced by 27.3%, or 8 t/ha/year. Thus, by implementing this land management technique, the basin's erosion rate may decrease from 29.33 to 21.33 t/ha/year (Figure 13). Contouring revealed results that were in opposition to the current study's findings when

conducted north of our study area and in various topography and soil conditions. In the Kalaya basin, cultivation parallel to contour lines simulation accelerated erosion rates, whereas terraces were classified in the first BMP class, and strip cropping was classified in the second (Briak et al., 2019).

Reforestation

This study used the SWAT model to simulate the hydrological response of selected sub-watersheds to changes in land use, with a particular focus on reforestation as a soil conservation measure. Sub-watersheds 21, 27, and 28 were identified as the most sediment-producing areas based on a spatial erosion risk assessment and the calibrated model's sediment yield outputs. To evaluate the potential impact of land use modification, a scenario-based simulation was conducted in which the current land cover, dominated by agricultural or bare land, was gradually replaced with forest cover within the model environment.

The SWAT model integrates land use data with soil and topographic characteristics to estimate sediment yield at the sub-watershed level using the modified universal soil loss equation (MUSLE). MUSLE accounts for runoff energy and peak flow when predicting erosion rates (Arnold et al., 1998;

Neitsch et al., 2011). Adjusting the land use inputs and rerunning the simulation under the reforestation scenario enabled the model to effectively capture the reduction in surface runoff and sediment detachment resulting from increased vegetation cover and root stability. As shown in Table 8, this approach significantly reduced erosion rates: by 22.2% in sub-watershed 21, by 21.8% in sub-watershed 27, and by 18.9% in sub-watershed 28. These results demonstrate that reforestation and revegetating high-erosion zones can substantially reduce sediment yield (Figure 13). This finding aligns with previous studies that highlight vegetation cover as one of the most influential factors in mitigating soil erosion (Gassman et al., 2007;

Pandey et al., 2009). The simulation supports the feasibility of nature-based solutions for erosion control, providing decision-makers with a cost-effective alternative to traditional structural measures, such as check dams or terracing. Thus, the SWAT modeling framework proves valuable in assessing land management scenarios and guiding sustainable watershed planning.

DISCUSSION

The SWAT model sensitivity analysis in this study revealed that V_CH_N2 and R_SOL_K parameters have the most significant impact on

Table 8. Predicted erosion values in sub-catchments following application of BMPs (values in bold refer to sub-catchments in which BMPs have been applied)

Sub-watershed	Current status	Terracing	Contouring	Strip cropping	Reforestation
1	18.59	18.59	18.59	18.59	16.11
2	16.34	16.34	16.34	16.34	17.70
3	8.42	8.42	8.42	8.42	8.95
4	15.16	15.16	15.16	15.16	15.62
5	6.84	6.84	6.84	6.84	6.27
6	12.31	12.31	12.31	12.31	12.79
7	9.62	9.62	9.62	9.62	9.04
8	7.07	7.07	7.07	7.07	5.76
9	8.38	8.38	8.38	8.38	9.26
10	30.00	4.06	17.63	8.63	30.68
11	11.16	11.16	11.16	11.16	11.08
12	5.36	5.36	5.36	5.36	4.39
13	16.58	16.58	16.58	16.58	15.21
14	18.42	18.42	18.42	18.42	17.17
15	10.00	10.00	10.00	10.00	9.88
16	11.94	11.94	11.94	11.94	10.92
17	5.36	5.36	5.36	5.36	5.44
18	13.38	13.38	13.38	13.38	12.77
19	18.53	18.53	18.53	18.53	18.54
20	17.49	17.49	17.49	17.49	16.15
21	52.19	5.33	25.61	12.75	39.99
22	21.18	2.92	13.71	6.84	13.15
23	63.29	7.97	43.24	21.65	63.78
24	59.16	7.88	41.60	20.81	60.72
25	99.86	13.21	59.91	29.88	89.30
26	50.52	6.53	32.31	16.13	43.74
27	21.99	3.29	13.74	6.70	17.24
28	80.90	9.76	40.97	20.36	62.90
29	71.14	10.86	52.12	26.02	72.92
30	64.87	9.17	46.45	23.21	65.46
31	63.29	8.11	42.89	21.43	63.65

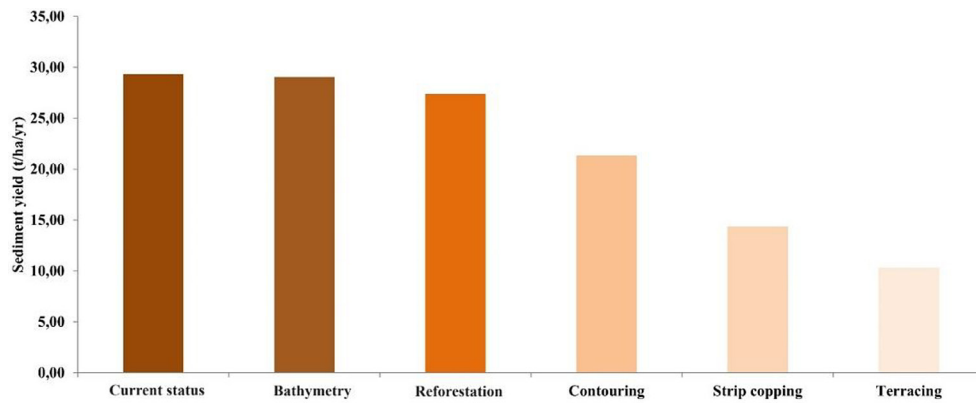


Figure 13. Simulated average annual sediment yield for different types of BMPs in the watershed (bathymetry corresponds to the siltation rate obtained by bathymetric measurements of the dam bottom)

flow rates. On the other hand, V_SPCON and V_SPEXP are more sensitive to sediment concentration. The investigation revealed that the sensitivity of both streamflow rates and sediment transport to the same set of factors has been observed in several Moroccan catchments with characteristics similar to those of our study regions. For example, the Kalaya watershed (Briak et al., 2016), the R'dom watershed (Brouziyne et al., 2018), the N'fis watershed (Markhi et al., 2019), and the Arbaa Ayacha watershed (Oualali et al., 2020). The objective functions used showed a significant and satisfactory fit in terms of model performance. Nevertheless, model performance is influenced by more than the parameters of sensitivity and by the target function. It is also influenced by the reliability of measurements (flow and sedimentation) from meteorological sites (Du et al., 2019) and the geographical location of these sites (Ricci et al., 2018). The four weather stations surrounding the basin provide little information on the geographical distribution of precipitation. Installation of a hydrometry station to measure sediment flux and concentration downstream of the basin. This site is spatially unsuitable to maximize model performance in most of the watershed. In fact, despite the lack of observations and rainfall events, some peaks in flow and sediment have been recorded in certain months. Similarly, SWAT was unable to detect smaller spikes (Ouallali et al., 2020).

In the context of the water balance, evapotranspiration plays a paramount role within the investigated region. This phenomenon is intricately linked to the presence of arid terrains and agricultural expanses. The intricate interplay of physical and chemical properties primarily dictates

the hydrological dynamics within the catchment. These attributes not only govern the generation of observed flow but also exert a significant influence on the spatial distribution of specific water constituents, particularly noteworthy in light of the prevalence of marl and clay lithology in the downstream segment of the basin, as elucidated by Ikenberry et al. (2017). The synergistic impact of lithological characteristics, slope gradients, and land use patterns amplifies surface runoff while concurrently imposing constraints on infiltration processes.

Furthermore, the incomplete consideration of water percolation through the soil to the groundwater table is acknowledged, given its potential contribution to flows beyond the basin's confines, as highlighted by Arnold et al. (1993). The anticipated repercussions of climate change introduce an additional layer of complexity to the partitioning of the water balance. The Moroccan Rif region, recognized as a focal point for climate change impacts (Beroho et al., 2020; Boulahfa et al., 2023), is anticipated to undergo significant alterations, including increased surface runoff, enhanced infiltration, recharged aquifers, and reduced evapotranspiration. The dominance of evapotranspiration and its relationship to land use and lithology are consistent with the model hydrological processes using SWAT with high-resolution data. The influence of marl and clay formations on runoff and infiltration supports the goal of investigating spatial variability in erosion and sedimentation processes. Acknowledging groundwater percolation highlights the need for improved calibration using long-term hydrological data, as outlined in the study's methodology. Including climate change impacts addresses the

objective of evaluating future challenges to the region's water resources. Together, these insights contribute to the development of sustainable management strategies for the Makhazine catchment and similar areas of Morocco.

The application of the SWAT model in this study yielded a computed mean annual sediment yield of 29.33 t/ha/yr, with peak and trough values reaching 99.86 t/ha/yr and 5.36 t/ha/yr, respectively. This concurs with analogous rates measured by bathymetric surveys in the basin and values observed in neighboring catchments (Kalaya and Arbaa Ayacha) (Briak et al., 2016; Ouallali et al., 2020), underscoring the model's robustness and adaptability to diverse hydrological contexts. The SWAT model also evaluated the effects of four BMPs on soil erosion and sediment yield in the El Makhazine basin, Morocco (terracing, strip cropping, contouring, and reforestation). Terracing was found to be the most effective BMP, followed by strip cropping, contour farming, and afforestation. Effectiveness varies depending on watershed slope, soil type, land use, and precipitation characteristics. The results of our study are consistent with results from other regions. The terraces act as physical barriers, slowing runoff and thus allowing sedimentation of suspended particles before they reach the dam. By channeling rainwater and reducing its speed, the terraces effectively limit the impact of erosion on the soils upstream, thus preserving the quality of the water stored in the dam. In addition, by reducing the flow of sediment, these practices help extend the duration of usefulness of dams by reducing siltation in reservoirs, thereby ensuring a continuous supply of water for various uses, from irrigation to domestic consumption (Briak et al., 2019; Zettam et al., 2022). Interestingly, cultivation parallel to the contour line showed a counterintuitive increase in erosion rates, emphasizing the site-specific nature of BMP effectiveness (Ahsan et al., 2023; Wang et al., 2022; Barrett et al., 2016; Briak et al., 2019) and highlighting the implications and limitations of the SWAT model and BMP simulation. This study finds that BMPs can reduce erosion and improve watershed management; however, these results require validation and verification using other methods and data.

The SWAT model's ability to replicate spatial variation in sediment and water yield dynamics throughout the Oued El Makhazine basin was significantly enhanced by the use of high-resolution (10 m) land-use/land-cover (LULC) and soil

maps (M'Barek et al., 2023). HRUs could be precisely delineated due to this fine-scale resolution, which captures critical small-scale factors that control runoff generation and sediment transport (Goulden et al., 2023), such as localized slopes prone to erosion, agricultural field boundaries, and soil variability. As a result, when compared to studies that used coarser inputs (such as ≥ 30 m) (Briak et al., 2019; Ouallali et al., 2020; Beroho et al., 2025), the model showed better accuracy in predicting sediment concentrations (e.g., $R^2 > 0.82$ for sediment calibration) and water production patterns. By resolving the effects of sensitive soil types (like vertisols) and land cover transitions (like deforestation to agriculture) on sediment loads at sub-catchment scales, the 10-m data resolution directly supported our goal of identifying targeted soil conservation strategies. This level of detail is not possible with datasets with lower resolution.

Despite the strengths of this study, certain limitations must be acknowledged. First, the limited availability and uneven distribution of hydrometeorological data, especially sediment concentration measurements, reduced the accuracy of model calibration. Second, the SWAT model does not explicitly simulate extreme precipitation events, which could impact erosion forecasts under changing climatic conditions. Future research should expand the monitoring network and incorporate remote sensing data to more accurately represent land use and precipitation. Additionally, integrating climate change scenarios into SWAT simulations would enhance the model's forecasting capabilities for long-term watershed planning.

This study contributes directly to several United Nations Sustainable Development Goals (SDGs), particularly SDG 6 (clean water and sanitation) and SDG 15 (life on land). By applying the SWAT model to assess hydrological processes and soil erosion dynamics in the El Makhazine catchment, the research supports improved water resource management and reduced land degradation, key targets under these SDGs. The identification and evaluation of best management practices (BMPs), particularly terracing, offer practical strategies for mitigating soil erosion, improving water quality, and extending the lifespan of reservoirs, which are crucial for sustainable agriculture and ecosystem conservation. Furthermore, by analyzing the impacts of climate, land use, and lithology on water balance components, this work offers a science-based foundation for

informed, climate-resilient watershed management. These insights are particularly relevant for regions facing similar environmental pressures, supporting global efforts toward sustainable development and resilience building in vulnerable agro-ecosystems.

CONCLUSIONS

This investigation examines the outcomes obtained from applying the Soil and Water Assessment Tool (SWAT) hydrological model to simulate the dynamics of the El Makhazine catchment from 1982 to 2018. A multi-objective optimization methodology was employed to calibrate and validate the model within the watershed meticulously. The evaluation of model performance was based on three distinct objective functions: Nash-Sutcliffe Efficiency (NSE), Percent Bias (PBIAS), and the coefficient of determination (R^2), resulting in both acceptable and satisfactory outcomes.

Optimal sensitivity parameters crucial for the study area were identified, primarily revolving around flow parameters such as CN2, ALPHA_BF, GW_DELAY, GWQMN, and CH_N2. Simultaneously, sediment-related parameters, including USLE_P, CH_COV1, USLE_K, SPCON, and CH_COV2, were identified as the most sensitive parameters, ensuring optimal model performance in capturing the hydrological complexities of the El Makhazine catchment. In the realm of erosion assessment, it is evident that a meticulous calibration and validation process has been conducted, incorporating a diverse set of performance metrics and objective functions. The computed average annual erosion rate is 29.33 t/ha/yr, with yearly variations ranging from 5.36 t/ha/yr to 99.86 t/ha/yr, demonstrating the model's robust performance across a wide range of conditions. The SWAT model, employed for computing water balance parameters, utilized average monthly values throughout the simulation period, resulting in a water yield ranging from 551.74 mm to 634.89 mm.

Within the study area, the preeminent component of the water balance is evapotranspiration, occupying the largest share in the basin, closely followed by surface runoff. The prevailing land use patterns, the temporal variability of rainfall, and, notably, the lithological attributes of substrates collectively contribute to the constrained infiltration capacity and heightened runoff observed in the region. In a comprehensive

assessment, the findings from the SWAT model application in the region exhibit promise and offer insights for formulating targeted anti-erosion measures. The model suggests that introducing terracing techniques within the basin could yield substantial reductions in erosion and siltation rates downstream. By adeptly characterizing sediment and water dynamics within the basin, the model emerges as a valuable tool for assessing water balance and sediment dynamics in the sub-humid watersheds of the Western Rif.

Acknowledgments

The authors would like to thank the anonymous reviewers who, through their comments and suggestions, helped us improve this paper. Our thanks also go to the Loukkos Hydraulic Basin Agency and the Maroc-Ingenov design office for their valuable help in preparing the data and verifying the results.

REFERENCES

1. Abbaspour, K.C. (2011). SWAT Calibration and uncertainty programs manual version 2, department of systems analysis, integrated assessment and modelling (SIAM), Eawag. *Swiss Federal Institute of Aquatic Science and Technology*, Duebendorf, Switzerland. 106. <https://doi.org/10.13031/2013.42256>
2. Abbaspour, K.C., Johnson, C.A., Van Genuchten, M.T. (2004). Estimating uncertain flow and transport parameters using a sequential uncertainty fitting procedure. *Vadose zone journal*, 3(4), 1340–1352. <https://doi.org/10.2113/3.4.1340>
3. Abbaspour, K.C., Rouholahnejad, E., Vaghefi, S.A.S., Srinivasan, R., Yang, H., Klöve, B. (2015). A continental-scale hydrology and water quality model for Europe: Calibration and uncertainty of a high-resolution large-scale SWAT model. *Journal of Hydrology*, 524, 733–752. <https://doi.org/10.1016/j.jhydrol.2015.03.027>
4. Abbaspour, K.C., Yang, J., Maximov, I., Siber, R., Bogner, K., Mieleitner, J., Zobrist, J., Srinivasan, R. (2007). Modelling hydrology and water quality in the pre-alpine/alpine Thur watershed using SWAT. *Journal of Hydrology*, 333(2–4), 413–430. <https://doi.org/10.1016/j.jhydrol.2006.09.014>
5. Abdulwahid, W.M., Pradhan, B., Jebur, M.N., Devkota, S. (2022). Soil erosion risk assessment using RUSLE, remote sensing, and GIS: A case study of Erbil District, Iraq. *Environmental Earth Sciences*, 81(12), 1–21. <https://doi.org/10.1007/s12665-022-10412-3>

6. Ahmadi, M., Minaei, M., Ebrahimi, O., Nikseresht, M. (2020). Evaluation of WEPP and EPM for improved predictions of soil erosion in mountainous watersheds: A case study of Kangir River basin, Iran. *Modeling Earth Systems and Environment*, 6, 2303–2315. <https://doi.org/10.1007/s40808-020-00814-w>
7. Ahsan, A., Das, SK., Khan, MHRB., Ng, AW., Al-Ansari, N., Ahmed, S., Shafiquzzaman, M. (2023). Modeling the impacts of best management practices (BMPs) on pollution reduction in the Yarra River catchment, Australia. *Applied Water Science*, 13(4), 98. <https://doi.org/10.1007/s13201-022-01812-2>
8. Ait M'Barek, S., Bouslihim, Y., Rochdi, A., Miftah, A. (2023). Effect of LULC data resolution on hydrological and erosion modeling using SWAT model. *Modeling Earth Systems and Environment*, 9(1), 831–846. <https://doi.org/10.1007/s40808-022-01537-w>
9. Al-hasn, R., Alghamaz, F., Dikkeh, M., Idriss, Y. (2024). Water soil erosion modeling with RUSLE, GIS & remote sensing: A case study of the AL-Sanaoubar River basin (Syria). *Journal of the Saudi Society of Agricultural Sciences*, 23(7), 474–484. <https://doi.org/10.1016/j.jssas.2024.05.004>
10. Arabi, M., Frankenberger, JR., Engel, BA., Arnold, JG. (2008). Representation of agricultural conservation practices with SWAT. *Hydrological Processes: International Journal*, 22(16), 3042–3055. <https://doi.org/10.1002/hyp.6890>
11. Arnold, JG., Allen, PM., Bernhardt, G. (1993). A comprehensive surface-groundwater flow model. *Journal of Hydrology*, 142(1–4), 47–69. [https://doi.org/10.1016/0022-1694\(93\)90004-S](https://doi.org/10.1016/0022-1694(93)90004-S)
12. Arnold, JG., Moriasi, DN., Gassman, PW., Abbaspour, KC., White, MJ., Srinivasan, R., Jha, MK. (2012). SWAT: Model use, calibration, and validation. *Transactions of the ASABE*, 55(4), 1491–1508. <https://doi.org/10.13031/2013.42256>
13. Arnold, JG., Srinivasan, R., Muttiah, RS., Williams, JR. (1998). Large area hydrologic modeling and assessment—Part I: Model development. *Journal of the American Water Resources Association*, 34(1), 73–89. <https://doi.org/10.1111/j.1752-1688.1998.tb05961.x>
14. Ayivi, F., Jha, MK. (2018). Estimation of water balance and water yield in the Reedy Fork-Buffalo Creek Watershed in North Carolina using SWAT. *International Soil and Water Conservation Research*, 6(3), 203–213. <https://doi.org/10.1016/j.iswcr.2018.03.007>
15. Banerji, US., Goswami, V., Joshi, KB. (2022). Quaternary dating and instrumental development: An overview. *Journal of Asian Earth Sciences*, X, 7, 100091. <https://doi.org/10.1016/j.jaesx.2022.100091>
16. Barrett, DC., and Frazier, AE. (2016). Automated method for monitoring water quality using Landsat imagery. *Water*, 8(6), 257. <https://doi.org/10.3390/w8060257>
17. Belasri, A., Lakhouili, A., Halima, OI. (2017). Soil erodibility mapping and its correlation with soil properties of Oued El Makhazine watershed, Morocco. *Journal of Materials and Environmental Sciences*, 8(9), 3208–3215. 340-JMES-3221-Belasri.pdf
18. Beroho, M., Aboumaria, K., El Hamdouni, Y., Oualali, A., Jaufer, L., Kader, S.,..., Briak, H. (2025). A novel SWAT-based framework to integrate climate and LULC scenarios for predicting hydrology and sediment dynamics in the watersheds of Mediterranean ecosystems. *Journal of Environmental Management*, 388, 125446. <https://doi.org/10.1016/j.jenvman.2025.125446>
19. Bodrud-Doza, M., Yang, W., De Queiroga Miranda, R., Martin, A., De Vries, B., Fraser, ED. (2023). Towards implementing precision conservation practices in agricultural watershed: A review of the use and prospects of spatial decision support systems and tools. *Science of The Total Environment*, 167118. <https://doi.org/10.1016/j.scitotenv.2023.167118>
20. Briak, H., Moussadek, R., Aboumaria, K., Mrabet, R. (2016). Assessing sediment yield in Kalaya gauged watershed (Northern Morocco) using GIS and SWAT model. *International Soil and Water Conservation Research*, 4(3), 177–185. <https://doi.org/10.1016/j.iswcr.2016.08.002>
21. Briak, H., Mrabet, R., Moussadek, R., Aboumaria, K. (2019). Use of a calibrated SWAT model to evaluate the effects of agricultural BMPs on sediments of the Kalaya River basin (North of Morocco). *International Soil and Water Conservation Research*, 7(2), 176–183. <https://doi.org/10.1016/j.iswcr.2019.02.002>
22. Chiang, LC., Shih, PC., Lu, CM., Jhong, BC. (2023). Strategies analysis for improving SWAT model accuracy and representativeness of calibrated parameters in sediment simulation for various land use and climate conditions. *Journal of Hydrology*, 626, 130124. <https://doi.org/10.1016/j.jhydrol.2023.130124>
23. De Oliveira Serrão, EA., Silva, MT., Ferreira, TR., de Ataíde, LCP., dos Santos, CA., de Lima, AMM., Gomes, DJC. (2022). Impacts of land use and land cover changes on hydrological processes and sediment yield determined using the SWAT model. *International Journal of Sediment Research*, 37(1), 54–69. <https://doi.org/10.1016/j.ijsrc.2021.04.002>
24. Djoukbala, O., Hasbaia, M., Benselama, O., Mazour, M. (2019). Comparison of the erosion prediction models from USLE, MUSLE and RUSLE in a Mediterranean watershed, case of Wadi Gazouana

- (NW of Algeria). *Modeling Earth Systems and Environment*, 5(2), 725–743. <https://doi.org/10.1007/s40808-018-0562-6>
25. Du, X., Shrestha, N.K., Wang, J. (2019). Assessing climate change impacts on stream temperature in the Athabasca River Basin using SWAT equilibrium temperature model and its potential impacts on stream ecosystem. *Science of the Total Environment*, 650, 1872–1881. <https://doi.org/10.1016/j.scitotenv.2018.09.344>
 26. Duru, U., Arabi, M., Wohl, E.E. (2018). Modeling stream flow and sediment yield using the SWAT model: a case study of Ankara River basin, Turkey. *Physical Geography*, 39(3), 264–289.
 27. Eltaif, N.I., Gharaibeh, M.A. (2022). Soil erosion catastrophe in Iraq-Preview, causes and study cases. *Environmental Degradation in Asia: Land Degradation, Environmental Contamination, and Human Activities*, 179–207. <https://doi.org/10.1080/002723646.2017.1342199>
 28. Forootan, E. (2023). GIS-based slope-adjusted curve number methods for runoff estimation. *Environmental Monitoring and Assessment*, 195(4), 489.
 29. Francesconi, W., Srinivasan, R., Pérez-Miñana, E., Willcock, S.P., Quintero, M. (2016). Using the soil and water assessment tool (SWAT) to model ecosystem services: A systematic review. *Journal of Hydrology*, 535, 625–636. <https://doi.org/10.1007/s10661-023-11039-6>
 30. Ganasri, B.P., Ramesh, H. (2016). Assessment of soil erosion by RUSLE model using remote sensing and GIS – A case study of Nethravathi Basin. *Geoscience Frontiers*, 7(6), 953–961. <https://doi.org/10.1016/j.gsf.2015.10.003>
 31. Gassman, P.W., Reyes, M.R., Green, C.H., Arnold, J.G. (2007). The soil and water assessment tool: Historical development, applications, and future research directions. *Transactions of the ASABE*, 50(4), 1211–1250. <https://doi.org/10.13031/2013.23637>
 32. Gassman, P.W., Reyes, M.R., Green, C.H., Arnold, J.G. (2007). The soil and water assessment tool: historical development, applications, and future research directions. *Transactions of the ASABE*, 50(4), 1211–1250. <https://doi.org/10.13031/2013.23637>
 33. Ghoraba, S.M. (2015). Hydrological modeling of the Simly Dam watershed (Pakistan) using GIS and SWAT model. *Alexandria Engineering Journal*, 54(3), 583–594. <https://doi.org/10.1016/j.aej.2015.05.018>
 34. Goharrokhi, M., McCullough, G.K., Lobb, D.A., Owens, P.N., Koiter, A.J. (2022). Sediment sources and transport dynamics in large, regulated river systems with multiple lakes and reservoirs in the subarctic region of Canada. *Hydrological Processes*, 36(9), e14675. <https://doi.org/10.1002/hyp.14675>
 35. Goulden, T., Jamieson, R., Hopkinson, C., Sterling, S., Sinclair, A., Hebb, D. (2014). Sensitivity of hydrological outputs from SWAT to DEM spatial resolution. *Photogrammetric Engineering & Remote Sensing*, 80(7), 639–652. <https://doi.org/10.14358/PERS.80.7.639>
 36. Guzman, J.A., Moriasi, D.N., Gowda, P.H., Steiner, J.L., Starks, P.J., Arnold, J.G., Srinivasan, R. (2015). A model integration framework for linking SWAT and MODFLOW. *Environmental Modelling & Software*, 73, 103–116. <https://doi.org/10.1016/j.envsoft.2015.08.011>
 37. Halbe, J., Pahl-Wostl, C., Adamowski, J. (2018). A methodological framework to support the initiation, design, and institutionalization of participatory modeling processes in water resources management. *Journal of Hydrology*, 556, 701–716. <https://doi.org/10.1016/j.jhydrol.2017.09.024>
 38. Halecki, W., Kruk, E., Ryzek, M. (2018). Loss of topsoil and soil erosion by water in agricultural areas: A multi-criteria approach for various land use scenarios in the Western Carpathians using a SWAT model. *Land use policy*, 73, 363–372. <https://doi.org/10.1016/j.landusepol.2018.01.041>
 39. Ikenberry, C.D., Crumpton, W.G., Arnold, J.G., Soupir, M.L., Gassman, P.W. (2017). Evaluation of existing and modified wetland equations in the SWAT model. *JAWRA Journal of the American Water Resources Association*, 53(6), 1267–1280. <https://doi.org/10.1111/1752-1688.12570>
 40. Jeyrani, F., Morid, S., Srinivasan, R. (2021). Assessing basin blue–green available water components under different management and climate scenarios using SWAT. *Agricultural Water Management*, 256, 107074. <https://doi.org/10.1016/j.agwat.2021.107074>
 41. Ketema, A., Dwarakish, G.S. (2021). Water erosion assessment methods: a review. *ISH Journal of Hydraulic Engineering*, 27(4), 434–441. <https://doi.org/10.1080/09715010.2019.1567398>
 42. Krysanova, V., & White, M. (2015). Advances in water resources assessment with SWAT—an overview. *Hydrological Sciences Journal*, 60(5), 771–783. <https://doi.org/10.1080/02626667.2015.1029482>
 43. Li, S., Cai, X., Emaminejad, S.A., Juneja, A., Niroula, S., Oh Singh, V. (2021). Developing an integrated technology-environment-economics model to simulate food-energy-water systems in Corn Belt watersheds. *Environmental Modelling & Software*, 143, 105083. <https://doi.org/10.1016/j.envsoft.2021.105083>
 44. Loveridge, M., Rahman, A. (2018). Monte Carlo simulation for design flood estimation: A review of Australian practice. *Australasian Journal of Water Resources*, 22(1), 52–70. <https://doi.org/10.1080/13241583.2018.1453979>

45. Matisoff, G. (2014). 210Pb as a tracer of soil erosion, sediment source area identification and particle transport in the terrestrial environment. *Journal of environmental radioactivity*, 138, 343–354. <https://doi.org/10.1016/j.jenvrad.2014.03.008>
46. Mengistu, AG., Van Rensburg, LD., Woyessa, YE. (2019). Techniques for calibration and validation of SWAT model in data scarce arid and semi-arid catchments in South Africa. *Journal of Hydrology: Regional Studies*, 25, 100621. <https://doi.org/10.1016/j.ejrh.2019.100621>
47. Moriasi, DN., Arnold, JG., Van Liew, MW., Binger, RL., Harmel, RD., Veith, TL. (2007). Model evaluation guidelines for systematic quantification of accuracy in watershed simulations. *Transactions of the ASABE*, 50(3), 885–900. <https://doi.org/10.13031/2013.23153>
48. Neitsch, SL., Arnold, JG., Kiniry, JR, Williams, JR. (2011). Soil and water assessment tool theoretical documentation version 2009. Texas Water Resources Institute.
49. Neitsch, SL., Arnold, JG., Kiniry, JR, Williams, JR., King, KW. (2005). Soil and water assessment tool theoretical documentation, version 2005. Temple, Tex.: USDA-ARS Grassland. Soil and Water Research Laboratory, 8.
50. Nourani, V., Singh, VP., Delafrouz, H. (2009). Three geomorphological rainfall–runoff models based on the linear reservoir concept. *Catena*, 76(3), 206–214. <https://doi.org/10.1016/j.catena.2008.11.008>
51. Oduor, BO., Campo-Bescós, MÁ., Lana-Renault, N., Kyllmar, K., Mårtensson, K., Casali, J. (2023). Quantification of agricultural best management practices impacts on sediment and phosphorous export in a small catchment in southeastern Sweden. *Agricultural Water Management*, 290, 108595. <https://doi.org/10.1016/j.agwat.2023.108595>
52. Ologunde, OH., Bello, SK., Busari, MA. (2024). Integrated agricultural system: A dynamic concept for improving soil quality. *Journal of the Saudi Society of Agricultural Sciences*, 23(5), 352–360.
53. O’Sullivan, JN. (2020). The social and environmental influences of population growth rate and demographic pressure deserve greater attention in ecological economics. *Ecological Economics*, 172, 106648. <https://doi.org/10.1016/j.jssas.2024.03.002>
54. Ouallali, A., Briak, H., Aassoumi, H., Beroho, M., Bouhsane, N., Moukhchane, M. (2020). Hydrological foretelling uncertainty evaluation of water balance components and sediments yield using a multi-variable optimization approach in an external Rif’s catchment. Morocco. *Alexandria Engineering Journal*, 59(2), 775–789. <https://doi.org/10.1016/j.aej.2020.02.017>
55. Pande, CB. (2020). Watershed management and development. *Sustainable Watershed Development: A Case Study of Semi-Arid Region in Maharashtra State of India*, 13–26. https://doi.org/10.1007/978-3-030-47244-3_2
56. Pandey, A., Chowdary, VM., Mal, BC. (2009). Identification of critical erosion-prone areas in the small agricultural watershed using GIS and remote sensing. *Water Resources Management*, 23(10), 1835–1859. <https://doi.org/10.1007/s11269-006-9061-z>
57. Parra, V., Fuentes-Aguilera, P., Muñoz, E. (2018). Identifying advantages and drawbacks of two hydrological models based on a sensitivity analysis: a study in two Chilean watersheds. *Hydrological Sciences Journal*, 63(12), 1831–1843. <https://doi.org/10.1080/02626667.2018.1538593>
58. Patra, S., Shilky Kumar, A., Saikia, P. (2023). Impact of land use systems and climate change on water resources: Indian perspectives. In *Advances in Water Resource Planning and Sustainability* 97–110. Singapore: Springer Nature Singapore. <https://doi.org/10.1007/978-981-99-3660>
59. Rahman, A., Weinmann, PE., Hoang, TMT., Laurenson, EM. (2002). Monte Carlo simulation of flood frequency curves from rainfall. *Journal of Hydrology*, 256(3–4), 196–210. [https://doi.org/10.1016/S0022-1694\(01\)00533-9](https://doi.org/10.1016/S0022-1694(01)00533-9)
60. Rast, M., Johannessen, J., Mauser, W. (2014). Review of understanding of Earth’s hydrological cycle: Observations, theory and modelling. *Surveys in Geophysics*, 35, 491–513. <https://doi.org/10.1007/s10712-014-9279-x>
61. Ravi, S., Breshears, DD., Huxman, TE., D’Odorico, P. (2010). Land degradation in drylands: interactions among hydrologic–aeolian erosion and vegetation dynamics. *Geomorphology*, 116(3–4), 236–245. <https://doi.org/10.1016/j.geomorph.2009.11.023>
62. Ricci, GF., De Girolamo, AM., Abdelwahab, OM., Gentile, F. (2018). Identifying sediment source areas in a Mediterranean watershed using the SWAT model. *Land degradation & development*, 29(4), 1233–1248. <https://doi.org/10.1002/ldr.2889>
63. Ricci, GF., Jeong, J., De Girolamo, AM., Gentile, F. (2020). Effectiveness and feasibility of different management practices to reduce soil erosion in an agricultural watershed. *Land Use Policy*, 90, 104306. <https://doi.org/10.1016/j.landusepol.2019.104306>
64. Rivas-Tabares, D., Tarquis, AM., Willaarts, B., De Miguel, Á. (2019). An accurate evaluation of water availability in sub-arid Mediterranean watersheds through SWAT: Cega-Eresma-Adaja. *Agricultural Water Management*, 212, 211–225. <https://doi.org/10.1016/j.agwat.2018.09.012>
65. Sadeghi, SHR., Gholami, L., Khaledi Darvishan, A., Saeidi, P. (2014). A review of the application of the MUSLE model worldwide. *Hydrological Sciences Journal*, 59(2), 365–375. <https://doi.org/10.1080/02626667.2013.866239>

66. Sahu, MK., Shwetha, HR., Dwarakish, GS. (2023). State-of-the-art hydrological models and application of the HEC-HMS model: a review. *Modeling Earth Systems and Environment*, 1–23. <https://doi.org/10.1007/s40808-023-01704-7>
67. Samimi, M., Mirchi, A., Moriasi, D., Ahn, S., Alian, S., Taghvaeian, S., Sheng, Z. (2020). Modeling arid/semi-arid irrigated agricultural watersheds with SWAT: Applications, challenges, and solution strategies. *Journal of Hydrology*, 590, 125418. <https://doi.org/10.1016/j.jhydrol.2020.125418>
68. Santos, F., Tevar, F., Andam, R., Baluyot, C., Robabo, V. (2022). Estimation of the Sediment Discharge of Marikina River Basin using Hydrologic Modeling System (HEC-HMS). In *2022 2nd International Conference in Information and Computing Research (iCORE)* 157–163. IEEE.
69. Sharma, A., Patel, PL., Sharma, PJ. (2022). Influence of climate and land-use changes on the sensitivity of SWAT model parameters and water availability in a semi-arid river basin. *Catena*, 215, 106298. <https://doi.org/10.1016/j.catena.2022.106298>
70. Silva, TP., Bressiani, D., Ebling, ÉD., Reichert, JM. (2024). Best management practices to reduce soil erosion and change water balance components in watersheds under grain and dairy production. *International soil and water conservation research*, 12(1), 121–136. <https://doi.org/10.1016/j.iswcr.2023.06.003>
71. Talebizadeh, M., Morid, S., Ahmed, K. (2020). Soil erosion assessment using GIS-based RUSLE in arid regions: A case study of the Shoor River Basin, Iran. *Arabian Journal of Geosciences*, 13(18), 1–12. <https://doi.org/10.1007/s12517-020-05899-w>
72. Uniyal, B., Dietrich, J., Vu, NQ., Jha, M., Arumí, JL. (2019). Simulation of regional irrigation requirement with SWAT in different agro-climatic zones driven by observed climate and two reanalysis datasets. *Science of the Total Environment*, 649, 846–865. <https://doi.org/10.1016/j.scitotenv.2018.08.248>
73. Vereecken, H., Amelung, W., Bauke, SL, Bogen, H., Brüggemann, N., Montzka, C., Zhang, Y. (2022). Soil hydrology in the Earth system. *Nature Reviews Earth & Environment*, 3(9), 573–587. <https://doi.org/10.1038/s43017-022-00324-6>
74. Verma, RK., Pandey, A., Mishra, SK. (2022). Curve numbers computation using observed rainfall-runoff data and RS and GIS-based NRCS-CN Method for direct surface runoff estimation in Tilaiya catchment. *Geospatial Technologies for Land and Water Resources Management*, 237–254. https://doi.org/10.1007/978-3-030-90479-1_15
75. Vervoort, W. (2017). Course Notes Advanced SWAT: Calibrating using SWAT-CUP. University of Sydney, IRI, INIA.
76. Walling, D., Foster, I. (2016). Using environmental radionuclides, mineral magnetism and sediment geochemistry for tracing and dating fine fluvial sediments. *Tools in fluvial geomorphology*, 181–209. <https://doi.org/10.1002/9781118648551>
77. Wang, Q., Liu, R., Men, C., Guo, L., Miao, Y. (2019). Temporal-spatial analysis of water environmental capacity based on the couple of SWAT model and differential evolution algorithm. *Journal of Hydrology*, 569, 155–166. <https://doi.org/10.1016/j.jhydrol.2018.12.003>
78. Wang, Y., Xu, HM., Li, Y.H., Liu, L.L., Hu, Z.H., Xiao, C., Yang, TT. (2022). Climate change impacts on runoff in the Fujiang River Basin based on CMIP6 and SWAT Model. *Water*, 14(22), 3614. <https://doi.org/10.3390/w14223614>
79. Worqlul, AW., Ayana, EK., Yen, H., Jeong, J., MacAlister, C., Taylor, R., Steenhuis, TS. (2018). Evaluating hydrologic responses to soil characteristics using SWAT model in a paired-watersheds in the Upper Blue Nile Basin. *Catena*, 163, 332–341. <https://doi.org/10.1016/j.catena.2017.12.040>
80. Yang, D., Yang, Y., Xia, J. (2021). Hydrological cycle and water resources in a changing world: A review. *Geography and Sustainability*, 2(2), 115–122. <https://doi.org/10.1016/j.geosus.2021.05.003>
81. Yang, J., Huang, ZC., Chen, TB., Lei, M., Zheng, YM., Zheng, GD., Zhang, C. (2008). Predicting the probability distribution of Pb-increased lands in sewage-irrigated region: a case study in Beijing, China. *Geoderma*, 147(3–4), 192–196. <https://doi.org/10.1016/j.geoderma.2008.08.014>
82. Yang, X., Liu, Q., He, Y., Luo, X., Zhang, X. (2016). Comparison of daily and sub-daily SWAT models for daily streamflow simulation in the Upper Huai River Basin of China. *Stochastic environmental research and risk assessment*, 30, 959–972. <https://doi.org/10.1007/s00477-015-1099-0>
83. Zettam, A., Briak, H., Kebede, F., Ouallali, A., Hallouz, F., Taleb, A. (2022). Efficiencies of best management practices in reducing nitrate pollution of the Sebdoou River, a semi-arid Mediterranean agricultural catchment (North Africa). *River Research and Applications*, 38(3), 613–624. <https://doi.org/10.1002/rra.3924>